J. Fluid Mech. (1991), *vol.* 226, *pp* 1–35
Printed in Great Britain

Measurements of particle dispersion obtained from direct numerical simulations of isotropic turbulence

By KYLE D. SQUIRES AND JOHN K. EATON
Department of Mechanical Engineering, Stanford University, Stanford, CA 94305, USA

(Received 24 November 1989 and in revised form 5 October 1990)

Measurements of heavy particle dispersion have been made using direct numerical simulations of isotropic turbulence. The parameters affecting the dispersion of solid particles, namely particle inertia and drift due to body forces were investigated separately. In agreement with the theoretical studies of Reeks, and Pismen & Nir, the effect of particle inertia is to increase the eddy diffusivity over that of the fluid (in the absence of particle drift). The increase in the eddy diffusivity of particles over that of the fluid was between 2 and 16%, in reasonable agreement with the increases reported in Reeks, and Pismen & Nir. The effect of a deterministic particle drift is shown to decrease unequally the dispersion in directions normal and parallel to the particle drift direction. Eddy diffusivities normal and parallel to particle drift are shown to be in good agreement with the predictions of Csanady and the experimental measurements of Wells & Stock.

1. Introduction

One of the most fascinating aspects of turbulent fluid motion is the greatly increased diffusion of scalar quantities suspended in it. These scalars may be smoke or dye which are able to follow all of the velocity fluctuations. However, these scalars may also be heavy particles which cannot follow all of the turbulent velocity fluctuations because of their finite inertia. This aspect of turbulent diffusion, i.e. the motion of heavy particles in a turbulent flow field, is made somewhat more complicated because of the additional parameters that enter into the problem. Prediction of these flows is important since particle-laden turbulent flows occur in many technologically important areas. Flows in energy conversion devices or problems in pollution control being two examples.

As originally shown by Corrsin (1961), the problem of turbulent diffusion is more suitably analysed in a reference frame that is attached to individual particles, i.e. a Lagrangian reference frame. Indeed, the first fundamentally correct theory of turbulent diffusion by G. I. Taylor (1921) is derived in a Lagrangian framework. The fact that turbulent diffusion is more suitable for analysis in a Lagrangian reference frame makes the problem less tractable using traditional laboratory measurements since these are made in the fixed Eulerian reference frame. Thus, one approach to solving problems of turbulent diffusion is to relate much more easily acquired Eulerian statistics to the Lagrangian quantities required for the theories. Examples of theories relating Lagrangian and Eulerian statistics include the work by Lumley (1961) equating the one-point moments of the Lagrangian and Eulerian probability density functions and Corrsin's conjecture (1959) expressing the Lagrangian velocity autocorrelation of fluid elements in terms of the two-point, two-time correlation of Eulerian velocities.

The theories of Taylor (1921) for isotropic turbulence and later extensions by Batchelor (1949) and Corrsin (1953) to homogeneous turbulence are equally applicable to heavy particle dispersion. The problem of heavy particle dispersion is more complicated than fluid point dispersion because of the lack of coincidence between the path of a heavy particle and the motion of a fluid element. Thus, additional dynamical equations must be solved to obtain the velocity field of the particle and its subsequent displacement. The first theoretical attempt at solving the equation of motion for a sphere in a turbulent flow to predict the dispersion of particles is that by Tchen (1947). Tchen linearized the equation of motion for a sphere in a turbulent flow in order to obtain expressions relating the eddy diffusivities of heavy particles to that of the fluid elements surrounding the particle. Unfortunately, the extremely restrictive assumptions made in order to solve the equation of motion make application of the results rather impractical for most problems of engineering interest. Lumley (1957) also used the equation of motion to analyse the dispersion characteristics of heavy particles and concluded that the problem could be resolved only on the level of functional probabilities.

For many applications of heavy particle dispersion the governing equation of particle motion may be greatly simplified. For example, if the density of the particle is much greater than the density of the carrier fluid (e.g. solid particles in air) then many of the forces in the equation of motion are negligible compared to the drag force. Furthermore, if the drag force obeys Stokes law then the equation of motion is linear in the velocity difference between fluid and particle. Thus, for many cases of practical interest the equation of motion for the particle is the linear drag term and also some imposed body force, typically gravity. Under these simplifying assumptions the principal effects influencing particle dispersion are inertia and drift.

It is well known that the deterministic drift of a particle through a turbulent flow field gives rise to a 'crossing-trajectories effect' which in turn reduces the dispersion of particles over that of the turbulence (Yudine 1959; Csanady 1963). It is also well known that the effect of crossing-trajectories reduces the dispersion of the particles unequally in directions parallel and normal to the direction of drift because of a related continuity effect. The effect of particle inertia on dispersion is not as clear since the particle eddy diffusivity is a function of its mean-square velocity and velocity autocorrelation. For increasing inertia the mean-square velocity fluctuations are decreased (thus decreasing the diffusivity) but the memory of the particle to its previous velocity is increased (thus increasing the diffusivity) and therefore the total effect on the particle diffusivity is not clear.

1.1. *Previous work and objectives*

The results from laboratory experiments are often difficult to interpret since the effects of inertia and particle drift are not always separated. Snyder & Lumley (1971) used a photographic technique to measure directly the Lagrangian velocity autocorrelations of individual particles in grid-generated isotropic turbulence. The results from this experiment showed that the velocity autocorrelations of heavy particles decreased faster than that of the light particles. Since the effects of inertia and drift were not isolated in this experiment the results were influenced by the crossing-trajectories effect. Wells & Stock (1983) performed a similar experiment in grid turbulence. In this experiment an electric field was imposed across the test section of the wind tunnel in order to cancel or enhance the effect of crossing-trajectories. In the absence of the crossing-trajectories effect, they found the asymptotic diffusivity to be weakly affected by particle inertia, though the

dispersion of heavy particles was slightly greater than that of light particles. Since it is often difficult to control the additional parameters in a laboratory experiment, effects such as uneven particle size or measurement errors can lead to results that are counter-intuitive. For example, Calabrese & Middleman (1979) examined the dispersion of particles in a turbulent pipe flow and their measurements showed the fluctuating velocities of the particles to be greater than that of the carrier fluid.

Theoretical approaches include work by Reeks (1977), who examined heavy particle dispersion in fluid velocity fields where the distribution of the fluid velocities was Gaussian, homogeneous, isotropic, stationary, and of zero mean. Reeks found that in the absence of particle drift the long-time particle diffusion coefficient was greater than that of the fluid for increasing values of the particle inertia. Pismen & Nir (1978) also examined particle dispersion assuming the characteristic function of the velocity field to be Gaussian and using Corrsin's 'independence approximation' (Corrsin 1959). Results from their study also showed that the particle eddy diffusivity increases for increasing particle inertia. Meek & Jones (1973) obtained expressions for the velocity autocorrelations, particle dispersion, and eddy diffusivities of particles using an assumed form for the Lagrangian velocity autocorrelation of the fluid. They obtained good agreement with Snyder & Lumley's data by stretching the frequency axis of the particle energy spectrum to account for particle drift. Maxey (1987) has examined the gravitational settling of aerosol particles in flow fields comprised of random Fourier modes and finds that the effect of particle inertia increases the settling velocity over the still-fluid value. Fung & Perkins (1989) have used a similar simulation technique to examine particle dispersion and find that in the absence of particle drift, the long-time eddy diffusivity of heavy particles is greater than that of the fluid.

While these previous efforts have provided some insight, additional information is required to increase the basic understanding of particle dispersion in turbulent flows. Laboratory experiments are often plagued by measurement uncertainties and difficulties isolating the effects influencing dispersion. Theoretical approaches often rely on simplifying assumptions that render the results of limited value. An alternative to increasing the basic understanding of particle dispersion in turbulent flows may be obtained using Direct Numerical Simulation (DNS) in which the Navier–Stokes equations are solved without resorting to turbulence modelling. The results from the simulation may be treated as experimental data with detailed time dependent measurements available at a large number of locations. Using DNS to obtain Lagrangian statistical information is also relatively straightforward since the necessary measurements are made following a particle path using suitable interpolation techniques. The use of DNS circumvents many of the previously mentioned difficulties associated with laboratory experiments and theoretical approaches but unfortunately is limited to low Reynolds number.

DNS was first used by Riley & Patterson (1974) to investigate particle dispersion in decaying isotropic turbulence. Using coarse grid computations (32^3) and a relatively small number of particles over which statistics were computed (432 particles) they measured particle dispersion, particle energies, and velocity autocorrelations. Their results showed that the velocity autocorrelation was increased for increasing values of particle inertia. Elghobashi & Truesdell (1989) have also used DNS to examine particle dispersion in decaying isotropic turbulence and report good agreement with the data of Snyder & Lumley. McLaughlin (1989) has examined particle deposition using DNS of channel flow and finds that particles tend to accumulate in the viscous sublayer. Recently, Squires & Eaton (1990) have used

DNS to investigate particle response to turbulence and modification of turbulence by particles. DNS has also been used by other investigators to obtain Lagrangian statistical data of fluid points (see Lee *et al.* 1988; Yeung & Pope 1989).

The results in this paper were obtained using DNS of both decaying and forced isotropic turbulence. Quantities such as time histories of particle energies, relative velocities, particle dispersion, velocity autocorrelations, and eddy diffusivities are presented. The effect of turbulence decay is investigated to determine its effect on heavy particle dispersion. The simulations of forced isotropic turbulence are useful for investigating particle dispersion since the analysis is not complicated by turbulence decay. Where possible the results have been compared to existing theories and in general the agreement is good.

2. Theory

The first fundamentally correct theory of turbulent diffusion was derived by Taylor (1921) for stationary isotropic turbulence. Batchelor (1949) and Corrsin (1953) extended the theory to homogeneous turbulence. In Taylor's theory the dispersion tensor for a single particle is expressed in terms of the particle velocity fluctuations and Lagrangian velocity autocorrelation:

$$\langle X_i(t)\,X_j(t)\rangle = \langle v_i^2\rangle^{\frac{1}{2}}\langle v_j^2\rangle^{\frac{1}{2}}\int_0^t\int_0^\tau [R_{ij}^{\mathrm{L}}(\xi)+R_{ji}^{\mathrm{L}}(\xi)]\,\mathrm{d}\xi\,\mathrm{d}\tau. \tag{2.1}$$

Throughout this paper repeated italic indices imply summation while repeated Greek indices are not summed. In (2.1) angle brackets denote ensemble averages, v_i is the component of the particle velocity in the ith direction and $R_{ij}^{\mathrm{L}}(\tau)$ is the autocorrelation of particle velocities. The velocity autocorrelation is defined as

$$R_{ij}^{\mathrm{L}}(\tau) = \frac{\langle v_i(t_0)\,v_j(t_0+\tau)\rangle}{\langle v_i^2\rangle^{\frac{1}{2}}\langle v_j^2\rangle^{\frac{1}{2}}}. \tag{2.2}$$

Notice that for statistically stationary turbulence the velocity autocorrelation is a function of only the time separation, τ.

As shown by Batchelor (1949), the dispersion tensor and Lagrangian velocity autocorrelation are related to the eddy diffusivity tensor through the following relations:

$$\begin{aligned} D_{ij}(t) &\equiv \frac{1}{2}\frac{\mathrm{d}}{\mathrm{d}t}\langle X_i(t)\,X_j(t)\rangle \\ &= \langle v_i^2\rangle^{\frac{1}{2}}\langle v_j^2\rangle^{\frac{1}{2}}\frac{1}{2}\int_0^t [R_{ij}^{\mathrm{L}}(\tau)+R_{ji}^{\mathrm{L}}(\tau)]\,\mathrm{d}\tau. \end{aligned} \tag{2.3}$$

Equation (2.3) illustrates that the eddy diffusivity is a time-dependent quantity, reaching a constant value only at long diffusion times.

Batchelor also introduced the spectral tensor, $E_{ij}^{\mathrm{L}}(\omega)$, which is the cosine transform of the velocity autocorrelation:

$$\langle v_i^2\rangle^{\frac{1}{2}}\langle v_j^2\rangle^{\frac{1}{2}}R_{ij}^{\mathrm{L}}(\tau) = \int_0^\infty E_{ij}^{\mathrm{L}}(\omega)\cos\omega\tau\,\mathrm{d}\omega. \tag{2.4}$$

The eddy diffusivity tensor may be expressed in terms of $E_{ij}^{\mathrm{L}}(\omega)$ as

$$D_{ij}(t) = \int_0^\infty E_{ij}^{\mathrm{L}}(\omega)\frac{\sin\omega t}{\omega}\,\mathrm{d}\omega. \tag{2.5}$$

Tchen (1947) linearized the equation of motion for a sphere in a turbulent flow and obtained expressions for the eddy diffusivities of particles and fluid. Tchen derived his theory for turbulence that is homogeneous and steady. Among the assumptions of his theory is that the particle is spherical and small enough such that its motion relative to the fluid follows Stokes law and the particle is small compared to the smallest turbulence lengthscales (i.e. the Kolmogorov scale). The most restrictive assumption in his theory is that during the motion of the particle the fluid surrounding the particle remains the same. This assumption implies that the fluid elements surrounding the particle are not distorted during the particle motion and that the particle does not 'overshoot' the fluid element surrounding the particle. However, for turbulent flows it is well known that fluid elements are continuously stretched and distorted and therefore the range of applicability of Tchen's theory is rather limited.

Given the assumptions Tchen uses to close this theory he finds that at short diffusion times

$$\frac{D_{\mathrm{p}\alpha\alpha}}{D^{\mathrm{p}}_{\mathrm{f}\alpha\alpha}} = \frac{\langle v_\alpha^2 \rangle}{\langle u_\alpha^2 \rangle} \tag{2.6}$$

where $D_{\mathrm{p}\alpha\alpha}$ is the diffusivity tensor of the heavy particles and $D^{\mathrm{p}}_{\mathrm{f}\alpha\alpha}$ is that of the fluid in the neighbourhood of the particle. The velocities of the particle and fluid in the vicinity of the particle are denoted v_α and u_α, respectively. For long diffusion times

$$\frac{D_{\mathrm{p}\alpha\alpha}}{D^{\mathrm{p}}_{\mathrm{f}\alpha\alpha}} = \frac{E^{\mathrm{L}}_{\mathrm{p}\alpha\alpha}(0)}{E^{\mathrm{pL}}_{\mathrm{f}\alpha\alpha}(0)} = 1. \tag{2.7}$$

Equations (2.6) and (2.7) give the short- and long-time asymptotes of the eddy diffusivity of the particles in terms of the eddy diffusivity of the fluid. For values of time between these asymptotes (2.3) may be used to determine the eddy diffusivity. However, as can be seen from (2.3) knowledge of the Lagrangian velocity autocorrelation of the particle velocity is required. An alternative to choosing a functional form of the velocity autocorrelation of the particles is to make use of the fact that the power spectrum of the particle velocities can be related to the power spectrum of the fluid velocities along the particle path through relations of the form

$$E^{\mathrm{L}}_{\mathrm{p}ij}(\omega) = \varpi^2 E^{\mathrm{pL}}_{\mathrm{f}ij}(\omega), \tag{2.8}$$

where ϖ is often referred to as the particle response function. For Stokes drag ϖ takes the form

$$\varpi(\omega) = \left[\frac{1}{1+\tau_{\mathrm{p}}^2\,\omega^2}\right]^{\frac{1}{2}}. \tag{2.9}$$

The form of the response function is modified if additional forces are included in the particle equation of motion (see Hinze 1975).

Since the velocity correlation of the fluid along the particle path, $R^{\mathrm{pL}}_{\mathrm{f}ij}(\tau)$, is the cosine transform of the power spectrum, $E^{\mathrm{pL}}_{\mathrm{f}ij}(\omega)$, assuming a functional form for $R^{\mathrm{pL}}_{\mathrm{f}ij}(\tau)$ allows determination of $E^{\mathrm{pL}}_{\mathrm{f}ij}(\omega)$ and then $E^{\mathrm{L}}_{\mathrm{p}ij}(\omega)$ through (2.8). Finally, given $E^{\mathrm{L}}_{\mathrm{p}ij}(\omega)$ the Lagrangian velocity autocorrelation of the particle is obtained through the use of the cosine transform relationship (equation (2.4)) and this can be used to determine the time-dependent nature of the diffusivity.

This approach has been used by Gouesbet, Berlemont & Picart (1984) in their analysis of turbulent dispersion of heavy particles. The functional form used for the velocity autocorrelation of the fluid along the particle path is

$$R_{tij}^{pL}(\tau) = \exp\left[\frac{-\tau}{(m^2+1)\,T_{Lij}^{p}}\right]\cos\left[\frac{m\tau}{(m^2+1)\,T_{Lij}^{p}}\right], \tag{2.10}$$

where T_{Lij}^{p} is the Lagrangian time integral scale tensor of the fluid along the particle path. This functional form was originally used by Frenkeil (1953). For $m = 0$ a simple decaying exponential form of the autocorrelation is obtained while for increasing values of m the correlation function given by (2.10) will have negative loops. Gouesbet showed that for values of m greater than 0, it is possible for the ratio $D_{pij}(t)/D_{tij}^{p}(\infty)$ to be larger than 1 for some values of time. Since their analysis uses the results of Tchen's theory as a starting point it should be remembered that the ratio $D_{pij}(t)/D_{tij}^{p}(\infty)$ will eventually be equal to 1 at long diffusion times. Thus, if $R_{tij}^{pL}(\tau)$ has negative loops it is possible that heavy particles will disperse faster than fluid elements for some values of time. Since Gouesbet's results are obtained in the framework of Tchen's theory it seems unlikely that the correlation function, $R_{tij}^{pL}(\tau)$, should have negative loops. This is because one of the assumptions in Tchen's theory is that the fluid neighbourhood surrounding the particle remains the same throughout the particle motion, i.e. the particle does not overshoot. In any case, Gouesbet argues that (2.10) should be used with $m = 1$ and it can be shown that particles may disperse faster than fluid elements.

It should also be remarked that the results obtained by Taylor (1921), Batchelor (1949) and others are applicable to turbulence that is homogeneous and statistically stationary. To apply these theories to the prediction of heavy particle dispersion requires that the velocity of a heavy particle be a stationary random variable. However, because of inertia the velocity of a heavy particle will exhibit an adjustment period following its release in which its velocity may not be considered a stationary function of time. Following this adjustment period the velocity of a heavy particle may be considered a stationary function and the relations outlined above are applicable for predicting the dispersion of heavy particles.

Finally, it is also important to emphasize that the results obtained by Tchen, Gouesbet, and others are derived in the absence of some externally imposed force field (e.g. gravity). Yudine (1959) and Csanady (1963) have shown that diffusivity of heavy particles is reduced over that of the fluid due to the crossing-trajectories effect.

3. Overview of the simulations

The three dimensional, time-dependent Navier–Stokes equations were solved for an incompressible fluid using the pseudo-spectral method originally developed by Rogallo (1981). This method is used to compute homogeneous turbulent flows and since homogeneous turbulence is in principle unbounded, numerical simulations of these flows employ periodic boundary conditions in a finite computational domain. Using a series representation the velocity field is expressed as a truncated Fourier series, i.e.

$$u_j(\boldsymbol{x}, t) = \sum_{\boldsymbol{k}} \hat{u}_j(\boldsymbol{k}, t) \exp(\mathrm{i}\boldsymbol{k}\cdot\boldsymbol{x}). \tag{3.1}$$

In (3.1) $u_j(\boldsymbol{x}, t)$ is the jth component of the velocity in physical space and $\hat{u}_j(\boldsymbol{k}, t)$ is the Fourier coefficient of u_j at wave vector $\boldsymbol{k}$. Substituting expressions such as that given by (3.1) into the Navier–Stokes equations and then applying the orthogonality property of $\exp(\mathrm{i}\boldsymbol{k}\cdot\boldsymbol{x})$ yields ordinary differential equations for $\hat{u}_j(\boldsymbol{k}, t)$. An advantage of using a series representation of the dependent variables is that extremely accurate

evaluation of spatial derivatives is possible because of the exponential convergence of the series (Gottlieb & Orszag 1977).

Evaluation of the nonlinear terms in a pseudo-spectral method is efficient since computation of these terms in physical space is less costly than in spectral or Galerkin methods. The transformation between wavenumber space and physical space can be accomplished efficiently using the fast Fourier transform algorithm (Cooley & Tukey 1965). Evaluation of the nonlinear terms in physical space gives rise to aliasing errors which are eliminated in the present code using a combination of coordinate shifts and truncation. The ordinary differential equations for the Fourier coefficients are time advanced using second-order Runge–Kutta. For further details of the method see Rogallo (1981) and Lee & Reynolds (1985).

3.1. *Properties of the Eulerian field*

Particle dispersion was investigated using simulations of decaying and forced isotropic turbulence. The simulations of decaying isotropic turbulence were performed using 128^3 points for the hydrodynamic computation while the simulations of forced isotropic turbulence were computed using 64^3 points. The computations were run on the Numerical Aerodynamic Simulation (NAS) facility Cray-2 supercomputer at the NASA-Ames Research Center.

The initial energy spectrum for the simulations of decaying isotropic turbulence was specified following the procedure of Lee & Reynolds (1985). Using this method of initialization the three-dimensional energy spectrum is specified as shown in (3.2):

$$E(k) = \begin{cases} Ck^2, & k_0 \leqslant k \leqslant k_\mathrm{p}, \\ \kappa \epsilon^{\frac{2}{3}} k^{-\frac{5}{3}}, & k_\mathrm{p} \leqslant k \leqslant k_\mathrm{max}, \\ 0, & \text{otherwise.} \end{cases} \tag{3.2}$$

In (3.2), k is the magnitude of the wavenumber vector and ϵ is the homogeneous dissipation rate. The maximum useful wave number is denoted k_max and is determined by the de-aliasing scheme. For Rogallo's code $k_\mathrm{max} = \frac{1}{3}\sqrt{2}N$ where N is the number of grid points in one direction. The lowest non-zero wavenumber is expressed as k_0 in (3.2). The constant κ for the spectrum has a value of approximately 1.5 (see Grant, Stewart & Moilliet 1962) and the value of C is obtained by matching the spectrum at $k = k_\mathrm{p}$. The wavenumber corresponding to the peak in the energy spectrum (k_p) for the simulations of decaying isotropic turbulence was 9.06.

The range of parameters from the simulations of decaying isotropic turbulence are summarized in table 1 where Re_λ is the Reynolds number based on twice the turbulence kinetic energy and Taylor microscale. For isotropic turbulence the Taylor microscale, λ, is given by the relation

$$\lambda = \left(\frac{5\nu}{\epsilon}\right)^{\frac{1}{2}} q. \tag{3.3}$$

The quantities q^2 and ϵ are twice the turbulence kinetic energy and homogeneous dissipation rate, respectively, and are determined from the three-dimensional energy spectrum:

$$\tfrac{1}{2}q^2 = \int_0^\infty E(k)\,\mathrm{d}k, \tag{3.4}$$

$$\epsilon = \nu \int_0^\infty k^2 E(k)\,\mathrm{d}k. \tag{3.5}$$

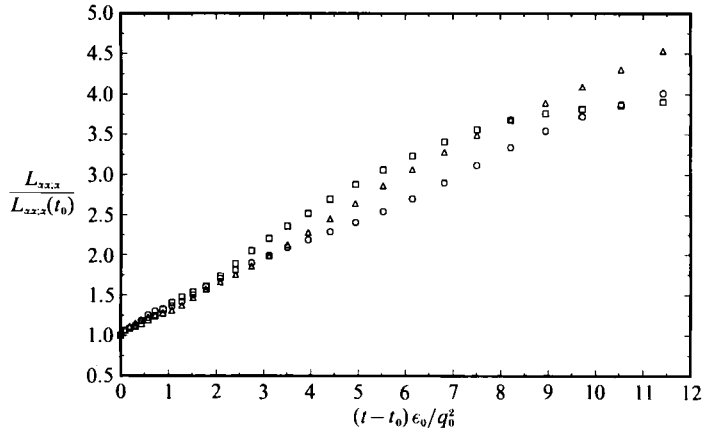

FIGURE 1. Time development of the longitudinal integral scales in decaying isotropic turbulence. □, $\alpha = 1$; ○, $\alpha = 2$; △, $\alpha = 3$.

Re_λ	Λ/L_{box}	$k_{\max}\eta$	t_s/τ_e
43.2 ~ 17.5	0.033 ~ 0.135	0.60 ~ 3.82	46.3

TABLE 1. Properties of the Eulerian field from simulations of decaying isotropic turbulence

The quantity Λ/L_{box} is the ratio of the integral lengthscale to the computational box size. The integral lengthscale, Λ, is calculated using the three-dimensional energy spectrum,

$$\Lambda = \frac{3\pi}{2q^2}\int_0^\infty \frac{E(k)}{k}\,\mathrm{d}k. \tag{3.6}$$

The duration of the simulations, t_s, has been non-dimensionalized by the eddy turnover time, τ_e, at $t = 0$ where τ_e is estimated as

$$\tau_e = \frac{\Lambda}{q}. \tag{3.7}$$

The Kolmogorov lengthscale is defined as

$$\eta = \left(\frac{\nu^3}{\epsilon}\right)^{\frac{1}{4}}. \tag{3.8}$$

The length of the computational box, L_{box}, was 2π for all simulations.

One check of isotropy from the simulations is the time development of the longitudinal integral scales. These lengthscales are obtained by integrating the area under the two-point spatial correlation,

$$L_{\alpha\alpha;\alpha} = \frac{1}{u_\alpha^2}\int_0^{\frac{1}{2}L_{\text{box}}} Q_{\alpha\alpha}(re_\alpha)\,\mathrm{d}r \quad (\alpha = 1,2,3), \tag{3.9}$$

where $Q_{ij}(\boldsymbol{r})$ is the two-point correlation defined by,

$$Q_{ij}(\boldsymbol{r}) \equiv \langle u_i(\boldsymbol{x})\, u_j(\boldsymbol{x}+\boldsymbol{r})\rangle \tag{3.10}$$

The integral scales defined by (3.9) are shown in figure 1. It can be seen from the figure that the integral scales are persistently isotropic throughout the simulation.

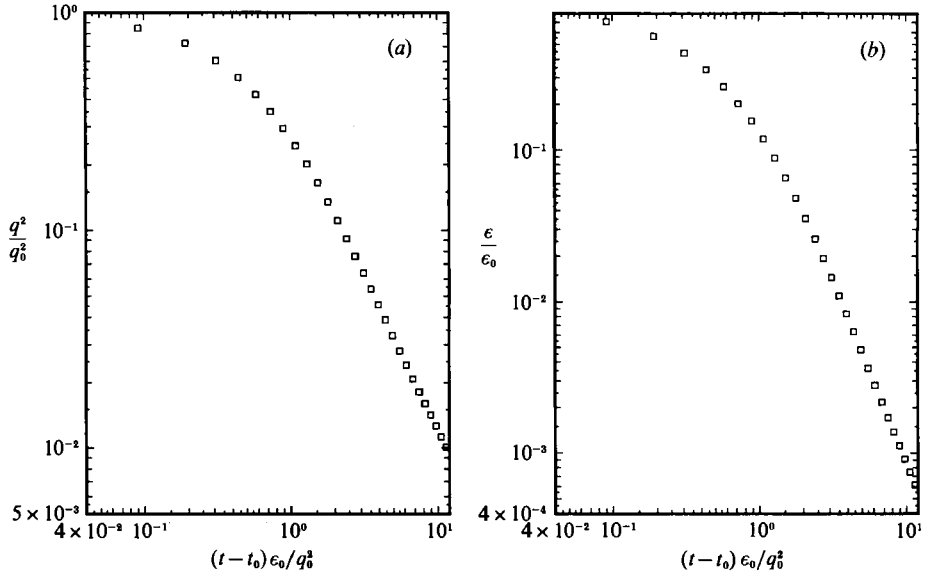

FIGURE 2. Time development of (*a*) twice the turbulence kinetic energy and (*b*) the homogeneous dissipation rate in decaying isotropic turbulence.

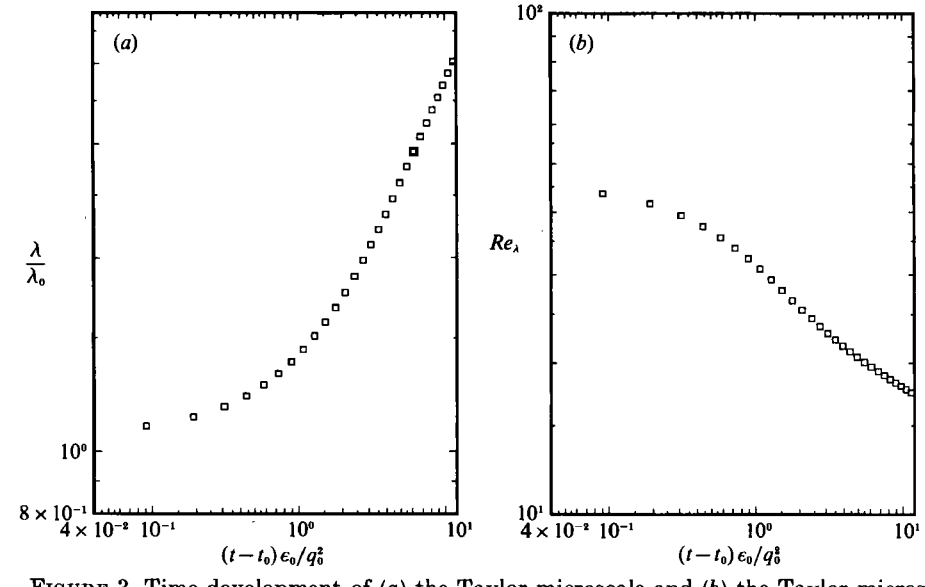

FIGURE 3. Time development of (*a*) the Taylor microscale and (*b*) the Taylor microscale Reynolds number in decaying isotropic turbulence.

Deviations from isotropy are probably due to the insufficient sample of large-scale motions. Integrals of the two-point correlations are quite sensitive to the sample of these motions.

The time development of twice the turbulence kinetic energy, the homogeneous dissipation rate, the Taylor microscale, and the microscale Reynolds number from the simulations of decaying isotropic turbulence are shown in figures 2 and 3. These figures show that after a short development period the turbulence energy and

Re_λ	Λ/L_{box}	$k_{max}\eta$	L_f/L_{box}	$q^2/(\epsilon\tau_e)$	$q^3/(\epsilon L_{box})$
38.7	0.126	1.41	0.184	4.34	1.29

TABLE 2. Properties of the Eulerian field from simulations of forced isotropic turbulence

dissipation decay with a nearly constant slope while the Taylor microscale shows an almost constant increase with respect to time when plotted in log–log coordinates.

Assuming the decay of the turbulence energy obeys a power law and that it is self-preserving implies

$$q^2 \approx \delta t^{-n}, \tag{3.11}$$

and turbulence lengthscales grow as

$$L_s \approx \delta t^{1-\frac{1}{2}n}. \tag{3.12}$$

The value of the decay exponent for q^2 is approximately 1.4. This exponent is in general agreement with the decay exponents obtained from simulations of isotropic turbulence by Lee & Reynolds (1985) and the experimentally determined values of Warhaft (1984) and Stapountzis *et al.* (1986). Warhaft obtained a decay exponent of 1.32 for the transverse fluctuations while Stapountzis *et al.* determined the decay exponent of the transverse velocity fluctuations to be 1.43. Using a value for the decay exponent of 1.4 for q^2, equation (3.12) would predict the turbulence lengthscales grow as $\delta t^{0.3}$. However, results from the simulations show the lengthscales grow more like $\delta t^{0.5}$ (e.g. see figure 3*a*). Thus the simulation data is not quite self-preserving, i.e. decay of the velocity scales is not precisely compensated by growth of the lengthscales. This is a characteristic of isotropic turbulence in the initial stage of decay (Hinze 1975).

Stationary isotropic turbulence was achieved by artificially forcing the low wavenumbers (large scales) at each timestep. The forcing scheme used for these simulations was developed by Hunt, Buell & Wray (1987). In this method a steady, non-uniform force field is introduced at the large scales of the flow. Starting from an arbitrary initial condition, a statistically stationary state is achieved after some time, in which the average rate of energy addition to the velocity field is equal to the average energy dissipation rate. The forcing coefficients are constrained to satisfy the continuity condition as well as isotropy of the velocity field. A description of the algorithm used to generate the forcing coefficients is contained in Appendix A.

After the Eulerian velocity field had evolved to a statistically stationary state, the Courant number ($U_{max}\Delta t/\Delta x$) was fixed so that time series data would be available at equally spaced time intervals. Lagrangian statistics were obtained only after the statistics of the turbulence field had become stationary. Table 2 summarizes the values of the hydrodynamic parameters in the 'developed' fields, i.e. after the calculation had reached a statistically stationary state. In table 2, L_f is the integral lengthscale obtained from the longitudinal velocity correlation ($\alpha = 1$ in equation (3.9).

The spatial energy and dissipation spectra from the simulations of forced isotropic turbulence are shown in figure 4. The energy spectra at wavenumber k are obtained by summing the magnitudes of the Fourier coefficients falling into a wavenumber band about k. These spectra were subsequently smoothed by multiplying by the ratio of the expected value of the modes in each band to the actual value contained therein (see Eswaran & Pope 1988 for further details). As is evident from the figures, a distinct peak in the spectra occur where the Fourier modes are forced.

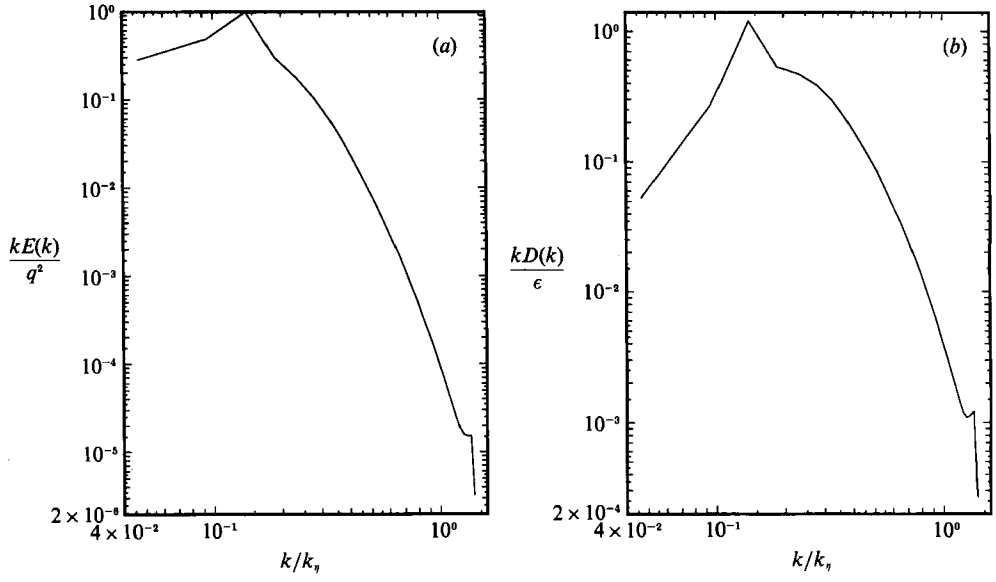

FIGURE 4. Three-dimensional spatial energy and dissipation spectra in forced isotropic turbulence.

3.2. *Particle parameters*

The particle equation of motion integrated in the simulations was

$$\frac{dv_i}{dt} = \alpha\left(u_i[X_j(t), t] - v_i(t) + \frac{g}{\alpha}\delta_{i2}\right) \tag{3.13}$$

where $X_j(t)$ and $v_i(t)$ are the position and velocity of the particle and g is the acceleration due to gravity. The quantity g/α is the Stokes settling velocity and is denoted v_{dr} throughout this work. The coefficient α is the inverse of the particle response time and assuming that the flow around the particle follows Stokes law of resistance is given by

$$\alpha = \frac{1}{\tau_p} = \frac{18\mu}{\rho_p d^2}. \tag{3.14}$$

In (3.14) μ is the dynamic viscosity of the carrier fluid, ρ_p is the particle density, and d is the particle diameter. Equation (3.13) represents a balance of the particle acceleration with the drag force and gravity. For α as given by (3.14) the drag force in (3.13) is assumed to obey Stokes law. This is appropriate if the Reynolds number based on the relative velocity between the particle and fluid is significantly less than one. The particle is also assumed to be smaller than the smallest lengthscales of the fluid flow field. For a turbulent flow this means that the particle diameter is smaller than the Kolmogorov microscale, η (Maxey & Riley 1983). It is also assumed the concentration of particles is small enough such that particle–particle interactions are negligible and the turbulence is not modified by the presence of the particles. Thus, the results in this paper apply to the dilute limit of particle-laden turbulent flows, e.g. dispersion of aerosols under most atmospheric conditions (Pruppacher & Klett 1978).

For each simulation the trajectories of as many as 4096 particles were tracked and the time histories of particle position and velocity as well as the fluid velocity in the

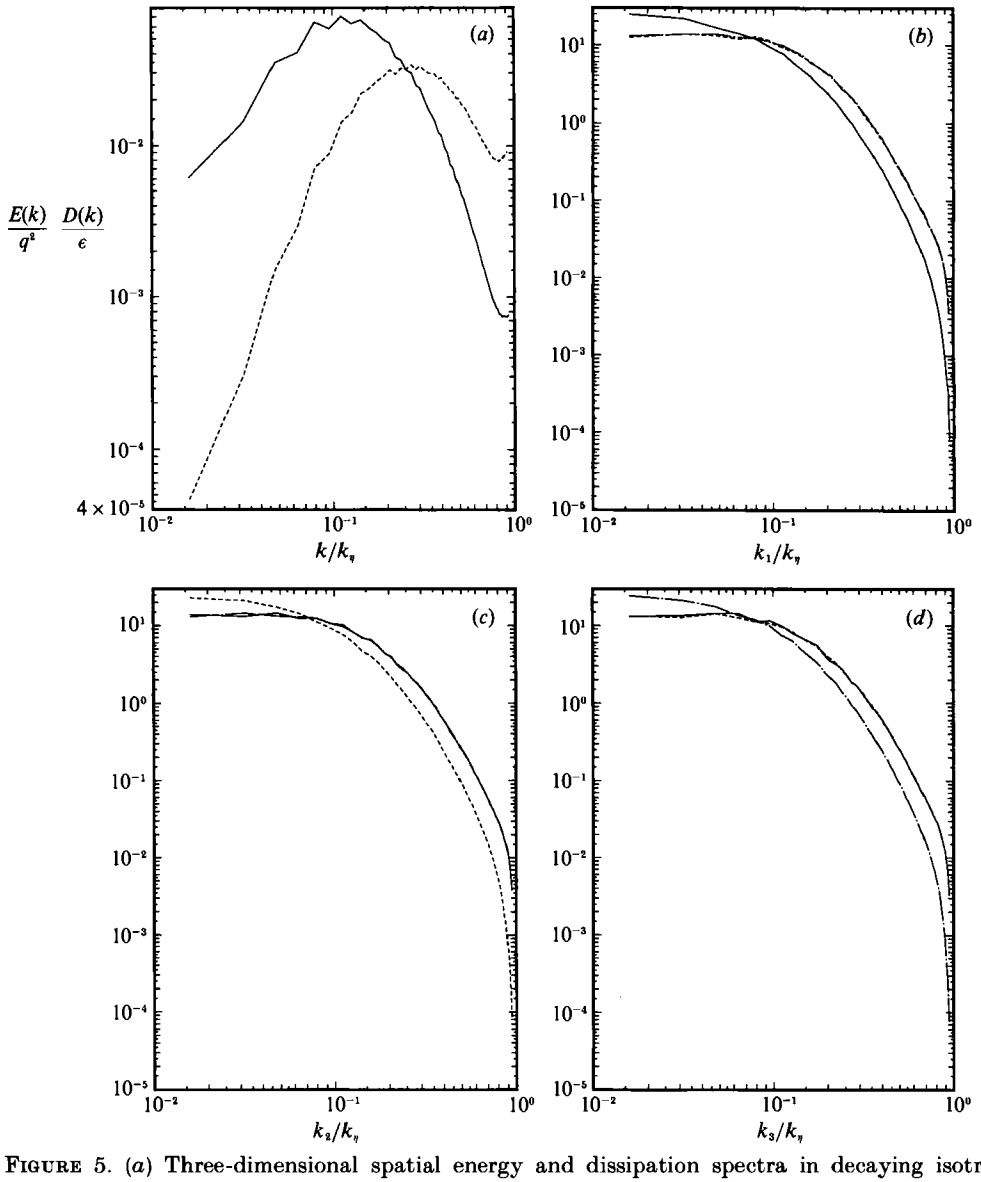

FIGURE 5. (*a*) Three-dimensional spatial energy and dissipation spectra in decaying isotropic turbulence, spectra shown correspond to first measurement of Lagrangian statistics. ——, $E(k)/q^2$; – – – –, $D(k)/\epsilon$. (*b*)–(*d*) One-dimensional energy spectra $E_{\alpha\alpha}(k_m)/(\epsilon\eta^5)^{\frac{1}{4}}$ in decaying isotropic turbulence, spectra shown correspond to first measurement of Lagrangian statistics. ——, $\alpha = 1$; – – – –, $\alpha = 2$; —·—, $\alpha = 3$.

Re_λ	Λ/L_{box}	$k_{max}\eta$	$\Delta T/\tau_e$
32.3	0.045	0.96	19.0
25.5	0.059	1.39	9.3

TABLE 3. Turbulence properties corresponding to initial and final measurement of Lagrangian statistics in decaying isotropic turbulence

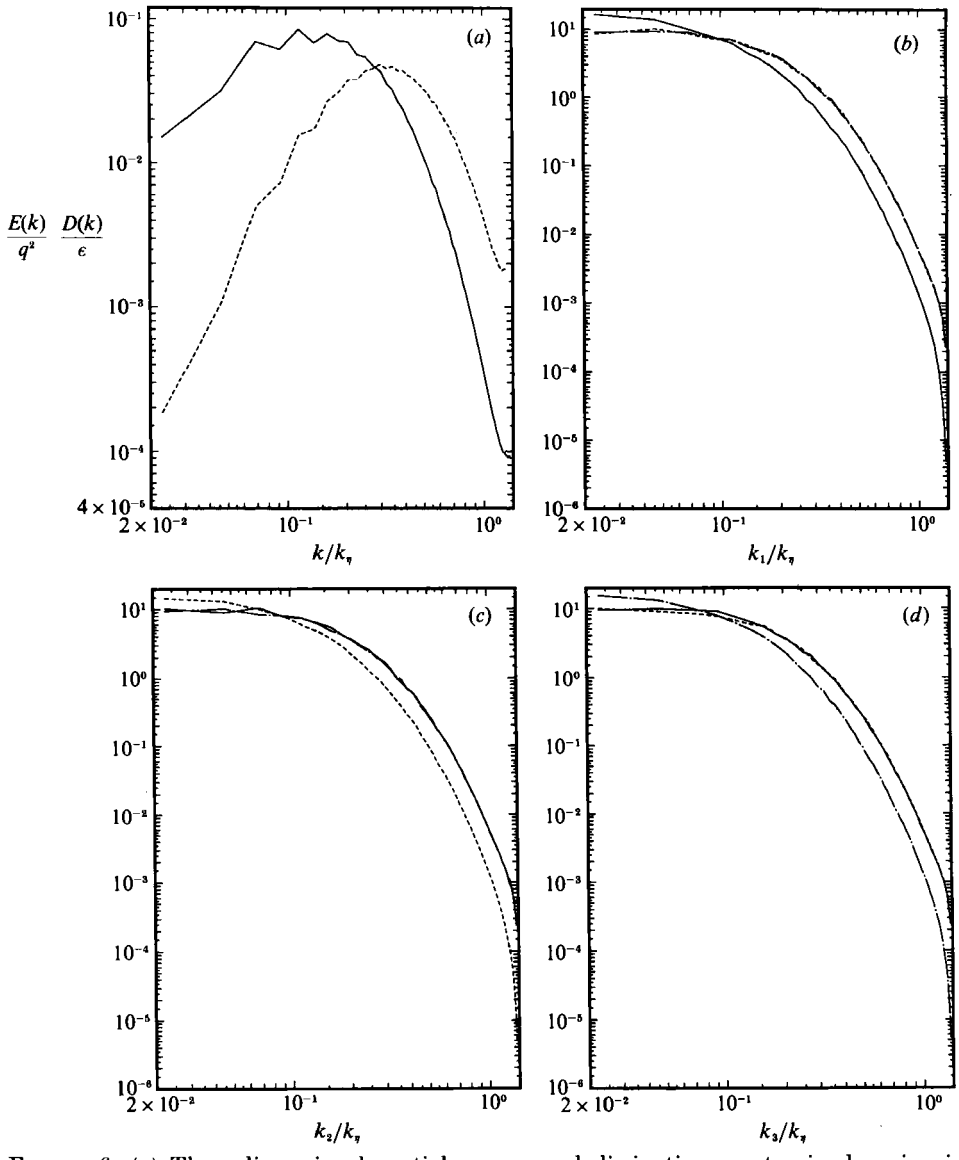

FIGURE 6. (*a*) Three-dimensional spatial energy and dissipation spectra in decaying isotropic turbulence, spectra shown correspond to final measurement of Lagrangian statistics. ——, $E(k)/q^2$; – – –, $D(k)/\epsilon$. (*b*)–(*d*) One-dimensional energy spectra $E_{\alpha\alpha}(k_m)/(\epsilon\eta^5)^{\frac{1}{4}}$ in decaying isotropic turbulence, spectra shown correspond to final measurement of Lagrangian statistics. ——, $\alpha = 1$; – – –, $\alpha = 2$; —·—, $\alpha = 3$.

vicinity of the particle were stored for later post-processing. Since it is only chance that a particle is located at a grid point (where the turbulence velocity is calculated) interpolation is required to obtain velocities of the turbulence along the particle trajectory. Both cubic splines and third-order accurate Lagrange polynomials were used to interpolate these velocities. It was found that more accurate interpolation techniques did not significantly improve the results. Since periodic boundary conditions are used for the hydrodynamic calculation there is no loss of accuracy of the interpolated particle properties when the particle is near a boundary.

τ_p/T_f	$\Delta T/\tau_p$	v_{dr}/u'
0.06	184	0.32
0.12	92	0.79
0.37	31	1.59
0.74	15	3.17
1.24	9	
3.72	3	

TABLE 4. Particle properties for decaying isotropic turbulence

After the turbulence had developed for a short time to eliminate the unphysical characteristics of the initial conditions the particles were time advanced using (3.13). For the simulations of decaying isotropic turbulence the particles were released once the skewness of the velocity derivative, $\partial u_\alpha/\partial x_\alpha$, had reached a threshold value corresponding to 'developed' turbulence. The value of the skewness of $\partial u_\alpha/\partial x_\alpha$ corresponding to developed turbulence is approximately -0.4 to -0.5 (see Lee & Reynolds 1985; Tavoularis, Bennett & Corrsin 1978) and the particles were released when the skewness had attained a value of -0.4. The particles used to obtain Lagrangian statistics in the simulations of forced isotropic turbulence were released once the turbulence had evolved to a statistically stationary state. The simulations of forced isotropic turbulence were then time advanced either 6 or 13 eddy turnover times. For all simulations the initial particle velocity was taken to be identical to the fluid velocity at the initial particle position and the initial distribution of particles throughout the computational box was uniform.

The Lagrangian data obtained from the simulations of decaying isotropic turbulence were computed using six reference times. The properties of the Eulerian field corresponding to the first and last reference time at which Lagrangian statistics were computed are summarized in table 3.

The one- and three-dimensional spatial spectra of the turbulence at the first and last reference times at which Lagrangian statistics were measured are shown in figures 5 and 6. The three-dimensional spectra in these figures show that the computation contains a reasonable sample of the large eddies and adequate resolution of the dissipative scales. The one-dimensional spectra demonstrate that both the large and small scales are isotropic.

Table 4 is a summary of the particle properties used for the simulations of decaying isotropic turbulence while the particle properties for the simulations of forced isotropic turbulence are contained in table 5. The particle time constant, τ_p, has been made dimensionless using the fluid timescale based on L_f and $u' = (\frac{1}{3}q^2)^{\frac{1}{2}}$ at the reference time of the measurement. This time scale is denoted T_f throughout this work. The particle drift velocity, v_{dr}, is non-dimensionalized using u' at the reference time of the measurement. The values of τ_p/T_f and v_{dr}/u' shown in table 4 correspond to the first reference time of the measurements. In tables 4 and 5, ΔT is the total length of time the particles were advanced in the simulation. It is important to note that in table 4 the values of τ_p/T_f are representative of simulations where the drift velocity, v_{dr}, of the particle was zero, i.e. these simulations were used to investigate the effect of particle inertia on dispersion. The values of the parameter v_{dr}/u' are for simulations where the effect of particle inertia is negligible.

τ_p/T_f	$\Delta T/\tau_p$	v_{dr}/u'
0.075	79	0
0.150	40	0
0.520	11	0
0.420	31	1.95
0.840	16	1.95

TABLE 5. Particle properties for forced isotropic turbulence

4. Dispersion in decaying isotropic turbulence

4.1. *Effect of particle inertia*

For the simulations of decaying isotropic turbulence it is important that Lagrangian statistics measured for the particles be computed only after the particles have become independent of their initial conditions. One measure of this independence is the mean-square relative velocity between fluid and particles, $\langle(u_i-v_i)^2\rangle$. Figure 7 shows the time history of this quantity (averaged over the components) for each of the values of τ_p used in the simulations (in the absence of particle drift). The time axis of all figures presented in §4 has been made dimensionless using the time required for the autocorrelation of fluid velocities to decrease to $1/e$ of its initial value. This timescale is denoted T_L^e. As would be expected, for increasing τ_p (increasing inertia) the influence of the initial condition of the particle velocity is more significant and more time is required to reach the peak in this quantity. The number of time constants required for each particle to reach the peak in the curves in figure 7 is shown in table 6.

Though it is not certain that the particles were independent of their initial conditions once the mean-square relative velocity had reached a maximum value, $\langle(u_i-v_i)^2\rangle$ does provide one indication that the particles are not overly influenced by their initial conditions. Thus, results from the simulations of decaying isotropic turbulence reported in this paper are computed after $\langle(u_i-v_i)^2\rangle$ had attained its maximum value.

Lagrangian autocorrelations of the particle velocities are shown in figure 8(*a*). These correlations were obtained from the simulations where only the inertia parameter was varied, i.e. in the absence of particle drift. It should be noted that the correlations shown for the simulations of non-stationary turbulence are computed as

$$R^L_{pij}(t_0,\tau) = \frac{\langle v_i(t_0)\, v_j(t_0+\tau)\rangle}{\langle v_i(t_0)^2\rangle^{\frac{1}{2}}\langle v_j(t_0+\tau)^2\rangle^{\frac{1}{2}}}, \tag{4.1}$$

where the average over $i = j = 1$, 2, and 3 are shown in figure 8(*a*) and the following figures unless otherwise noted and t_0 corresponds to a time in the simulation following the peak in the mean-square relative velocity. The normalization in (4.1) lessens the effect on the correlation of the reference time of the measurement, t_0 (Squires & Eaton 1991). Shown for comparison in figure 8(*a*) is the velocity autocorrelation of fluid points which exactly track the turbulent fluctuations. As can be seen from the figure, the 'memory' of the particle to its previous velocity is increased as the particle inertia increases, thus increasing the correlation coefficient over that for fluid particles. It may also be seen that at later times the correlations of the heavy particles cross over that of the fluid points. Thus, at long times the particle velocities are less correlated than the fluid. It is also evident from figure 8(*a*) that the

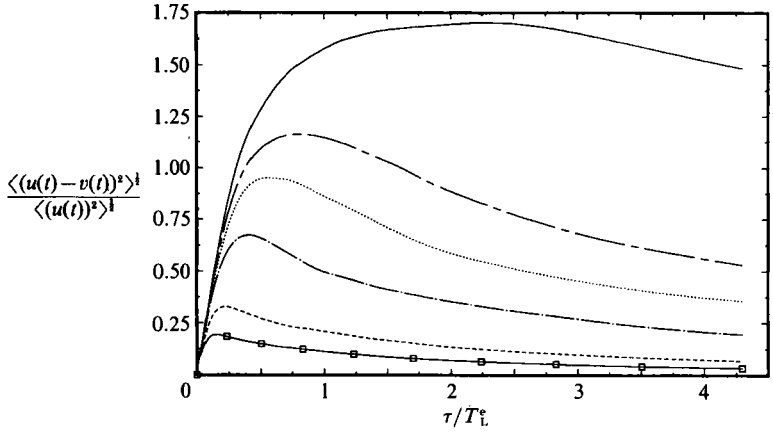

FIGURE 7. Time development of the relative velocity in decaying isotropic turbulence. □——□, $\tau_p/T_f = 0.06$; ----, $\tau_p/T_f = 0.12$; —·—, $\tau_p/T_f = 0.37$; ·····, $\tau_p/T_f = 0.74$; ———, $\tau_p/T_f = 1.24$; ——, $\tau_p/T_f = 3.72$.

τ_p/T_f	$\Delta t_{peak}/\tau_p$
0.06	2.13
0.12	1.57
0.37	0.92
0.74	0.61
1.24	0.44
3.72	0.20

TABLE 6. Number of time constants required to reach peak in $\langle(u_i-v_i)^2\rangle$

correlations do not decrease to zero at long separation times. This is presumably due to the decay of the turbulent fluctuations with time and the normalization used in (4.1).

Figure 8(*b*) shows the correlations of fluid velocities along the particle path. Shown for comparison in this figure are the temporal correlations of fluid velocities measured at fixed points in space, i.e. independent of particle motion. This figure shows that at short times the correlation of the fluid velocity along the path of the heavier particles decreases more rapidly than does that of the lighter particles. This would seem to be caused by the heavier particles 'overshooting' the fluid particle paths. Particles that overshoot fluid trajectories encounter low-frequency fluctuations of the fluid more often than do lighter particles, which are better able to follow the fluid trajectories. This is not unlike the advection hypothesis of Tennekes (1975) which is based on arguments that frequencies measured in the Eulerian frame will be higher than those in the Lagrangian reference frame because of advection of the small eddies by the large scales past a measuring point. Often, this effect is not observed in calculations that approximate the turbulent velocity field using random Fourier modes since these calculations do not account for the nonlinear interactions of the advective terms in the Navier–Stokes equations (e.g. see Riley 1971). Tennekes' analysis predicts that the Eulerian time microscale will be much lower than the Lagrangian time microscale (for fluid elements). However, results from these simulations are not in good agreement with his theory, possibly due to the low Reynolds numbers of the simulations.

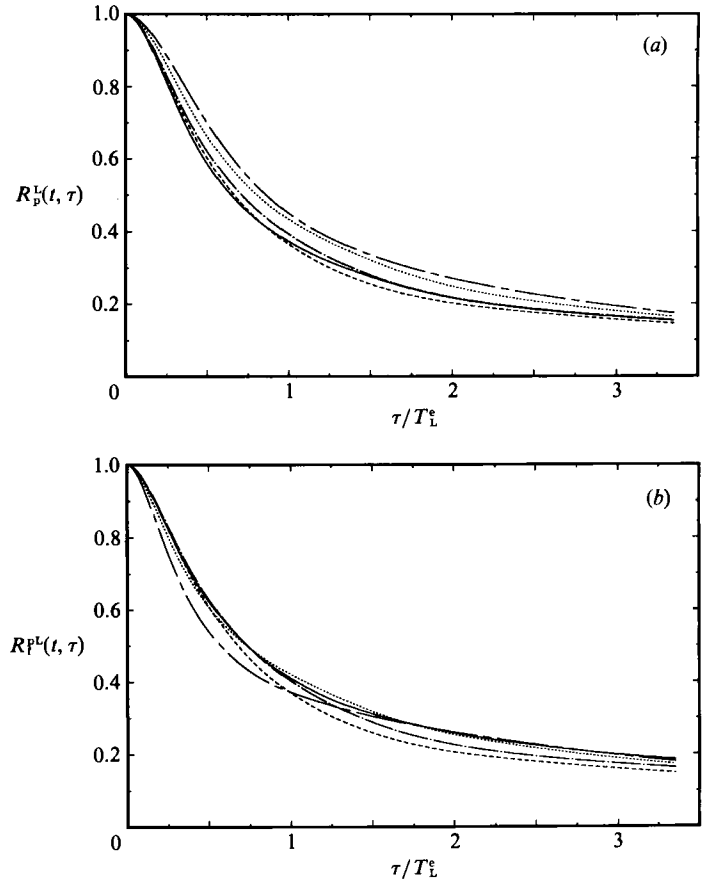

FIGURE 8. (*a*) Effect of inertia on the particle velocity correlation, $Re_\lambda = 25.5$. ——, fluid; – – – –, $\tau_p/T_f = 0.03$; —·—, $\tau_p/T_f = 0.06$, · · · · · · · · ·, $\tau_p/T_f = 0.18$; — — —, $\tau_p/T_f = 0.35$. (*b*) Effect of inertia on fluid velocity correlations along particle path, $Re_\lambda = 25.5$. ——, fixed point; – – – –, $\tau_p/T_f = 0.03$; —·—, $\tau_p/T_f = 0.06$; · · · · · · · · ·, $\tau_p/T_f = 0.18$; — — —, $\tau_p/T_f = 0.35$.

The effect of particle inertia on dispersion, $\langle X^2(t)\rangle$, is shown in figure 9(*a*). The dispersion shown in this figure has been non-dimensionalized by T_L^e and u' for fluid particles at the reference time of the measurement. This figure shows that for increasing particle inertia the dispersion also increases, except for the largest value of τ_p used in the simulations ($\tau_p/T_f = 0.35$). These dispersion measurements were used to compute the eddy diffusivity of the particles using (2.3). The eddy diffusivities of the particles are shown in figure 9(*b*) which shows that for all values of the particle inertia the eddy diffusivity is greater than that of fluid particles. It may also be seen from the figure that the diffusivity increases for increasing values of the particle inertia. The particles with the largest inertia, $\tau_p/T_f = 0.18$, $\tau_p/T_f = 0.35$, have asymptotic values of the eddy diffusivity which are nearly identical and roughly 10% greater than that of the fluid. From (2.3) it can be seen that at long diffusion times, for stationary turbulence, the eddy diffusivity will reach a constant value. Figure 9(*b*) shows that even for decaying isotropic turbulence the eddy diffusivity reaches an asymptotic value that is nearly time independent. This is because the diffusivity is proportional to a lengthscale squared and the inverse of a timescale. For decaying isotropic turbulence the lengthscale grows nearly as $t^{\frac{1}{2}}$ while

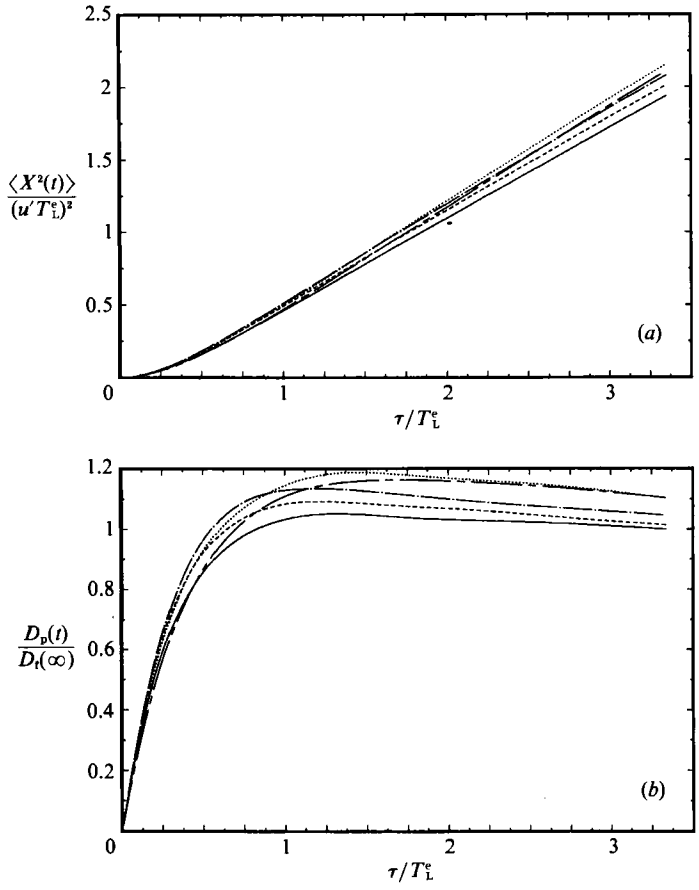

FIGURE 9. (*a*) Effect of inertia on particle mean-square displacement, $Re_\lambda = 25.5$. ——, fluid; – – –, $\tau_p/T_f = 0.03$; —·—, $\tau_p/T_f = 0.06$; · · · · · · · · ·, $\tau_p/T_f = 0.18$; — — —, $\tau_p/T_f = 0.35$. (*b*) Effect of inertia on particle eddy diffusivity, $Re_\lambda = 25.5$. ——, fluid; – – –, $\tau_p/T_f = 0.06$; · · · · · · · · ·, $\tau_p/T_f = 0.18$; — — —, $\tau_p/T_f = 0.35$.

the timescale grows nearly as t. Thus, the net effect is that the asymptotic diffusivity is nearly constant. From figure 9(*b*) the region in which the eddy diffusivity becomes approximately time independent occurs for time separations greater than about $2T_L^e$. For $t > 2T_L^e$ the particle eddy diffusivity is 2–10 % greater than that of the fluid. The result that, in the absence of a deterministic drift, the particle eddy diffusivity is greater than that of the fluid has also been reported by Reeks (1977) and Pismen & Nir (1978). The increases in the particle diffusivity relative to that of the fluid found in these studies is comparable to the increases reported here. A quantitative comparison of the ratio of the particle to fluid eddy diffusivity is made in §5.

Finally, it should be remarked that since the turbulence decays nearly self-similarly, it is possible to rescale the variables such that the resulting statistics are representative of stationary turbulence. This approach was introduced by Taylor (1935) and has been applied by other investigators to data obtained from grid turbulence experiments (e.g. see Townsend 1954; Snyder & Lumley 1971; Shlien & Corrsin 1974). While rescaling has been demonstrated to be successful for fluid element diffusion the application of a similar analysis to the data of heavy particle dispersion may not be appropriate since the timescales and lengthscales experienced

by the particle during its motion may not follow the same decay laws as experienced by a wandering fluid particle. Therefore, the dispersion measurements of heavy particles presented in this study were not re-scaled to account for turbulence decay. The reader is referred to Nir & Pismen (1979) for further discussion.

4.2. *Effect of particle drift*

The results presented in this section illustrate the effect of a deterministic particle drift velocity on dispersion quantities. Since it is desired to examine the effect of particle drift on the results, the particle inertia is considered negligible. Thus, the particle velocity is the sum of the fluid velocity in the vicinity of the particle plus its drift velocity,

$$v_i(t) = u_i[X_j(t), t] + v_{\mathrm{dr}}. \tag{4.2}$$

For the results presented here the drift velocity was non-zero in the y (x_2)-direction. Since the particle velocity given by (4.2) is independent of a particle time constant there is no adjustment period in which the particles become independent of their initial conditions. Thus, nearly all of the results presented in this section were obtained from the first reference time of the measurements.

The effect of increasing drift velocity on the particle velocity correlation components is illustrated in figure 10(a, b). For comparison the velocity correlations of fluid elements are also shown. It is evident from the figures that for increasing values of the drift velocity the autocorrelation decreases more rapidly. These results are consistent with Yudine's (1959) and Csanady's (1963) physical ideas concerning loss of correlation due to a crossing-trajectories effect and associated continuity effect. That is, as the drift velocity of a particle is increased it crosses the paths of fluid elements more rapidly and will tend to lose correlation with its previous velocity faster than will a fluid element.

The components of the Lagrangian velocity autocorrelation for one value of the drift velocity are shown in figure 10(c). These curves are representative of those obtained from the simulations of decaying isotropic turbulence. As is evident from the figure, the correlation of velocities along the drift direction, $R^{\mathrm{L}}_{\mathrm{p}22}(t, \tau)$, is more persistent than the correlations of velocities perpendicular to the direction of drift. This figure helps to show an effect associated with that of crossing trajectories referred to as the continuity effect (Csanady 1963). This effect arises when considering the dispersion of particles in which the drift velocity is large relative to the turbulent fluctuations. For rapid fallout of particles the Lagrangian velocity autocorrelation of a heavy particle will be very similar to that of an Eulerian space–time correlation. Thus, the Lagrangian correlation of particle velocities along the drift direction may be expressed as

$$R^{\mathrm{L}}_{\mathrm{p}22}(\tau) \approx \tilde{R}^{\mathrm{E}}_{22}(\tau, -v_{\mathrm{dr}}\tau), \tag{4.3}$$

where $\tilde{R}^{\mathrm{E}}_{22}$ is the fluid space–time correlation measured in the Eulerian reference frame

$$\tilde{R}^{\mathrm{E}}_{22}(\tau, -v_{\mathrm{dr}}\tau) = \frac{\langle v(t, y)\, v(t+\tau, y - v_{\mathrm{dr}}\tau)\rangle}{\langle v^2\rangle}. \tag{4.4}$$

Notice that for homogeneous turbulence there is no dependence of the correlation on x or z.

If the fallout velocity is sufficiently rapid the time delay in (4.4) may be neglected. For this case the expression for $\tilde{R}^{\mathrm{E}}_{22}$ reduces to the two-point spatial correlation of

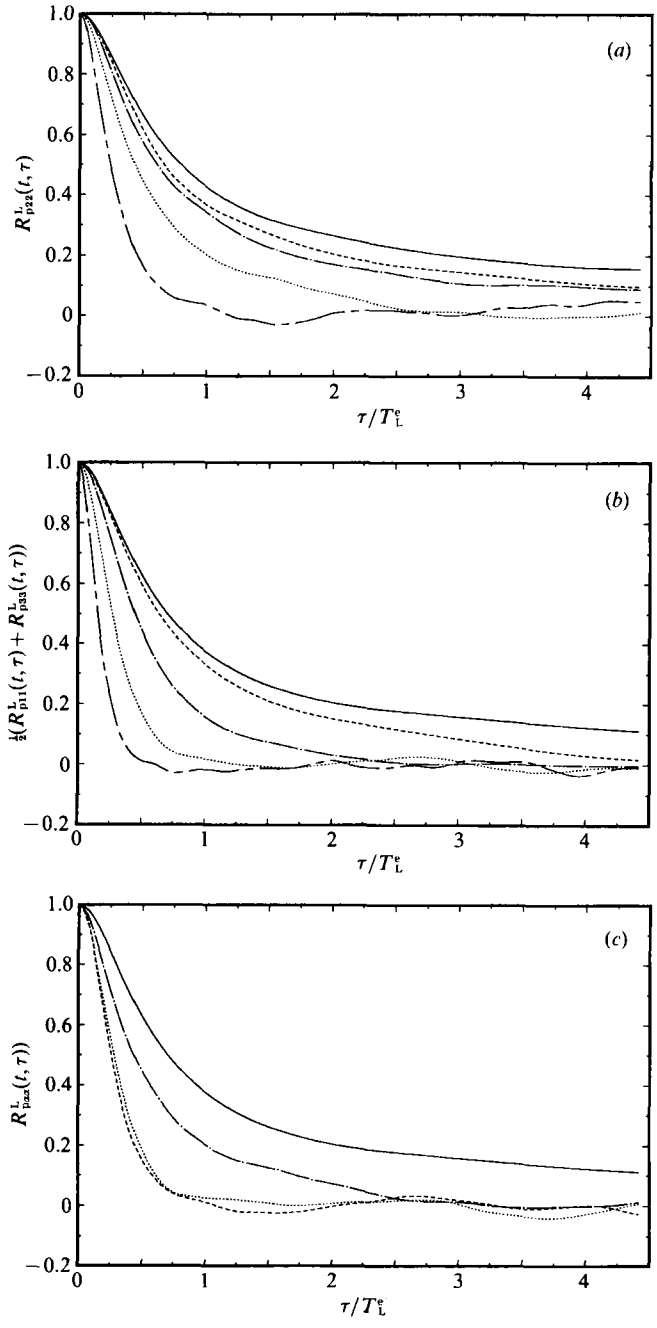

FIGURE 10. Effect of drift on the particle velocity correlation, $Re_\lambda = 32.3$. (*a*) Drift component. (*b*) Normal components. ——, fluid; – – –, $v_{dr}/u' = 0.32$; —·—, $v_{dr}/u' = 0.79$; · · · · · · · · ·, $v_{dr}/u' = 1.59$; — — —, $v_{dr}/u' = 3.17$. (*c*) Components of the Lagrangian velocity correlation. $Re_\lambda = 32.3$, $v_{dr}/u' = 1.59$. ——, fluid, – – –, $\alpha = 1$; —·—, $\alpha = 2$; · · · · · · · · ·, $\alpha = 3$.

Eulerian velocities. Thus, in this limiting case the correlations of the particle velocities along the drift direction are nearly identical to the two-point spatial correlation of longitudinal velocities measured in the Eulerian reference frame. Furthermore, the correlation of velocities perpendicular to the drift direction may be

approximated by the two-point correlation of lateral velocities. These correlations of lateral velocities must contain negative regions since the continuity constraint requires them to satisfy

$$\iint \tilde{R}_{11}^{\mathrm{E}}\,\mathrm{d}x_1\,\mathrm{d}x_3 = 0, \tag{4.5a}$$

and

$$\iint \tilde{R}_{33}^{\mathrm{E}}\,\mathrm{d}x_1\,\mathrm{d}x_3 = 0. \tag{4.5b}$$

Thus, it should be expected that for large values of the particle drift velocity the correlations of velocities perpendicular to the drift direction will be decreased over those along the drift direction. This effect may be seen for all values of the drift velocity by comparing figures 10(*a*) and 10(*b*). These figures also show the difference between the correlations increasing as the drift velocity increases.

Csanady also derived expressions for the components of the diffusivity tensor both perpendicular and parallel to the drift direction. Assuming an exponential form for the velocity correlations Csanady obtained

$$\frac{(D_{\mathrm{p1}}+D_{\mathrm{p3}})}{2D_{\mathrm{p2}}} = \frac{(1+(\beta^2 v_{\mathrm{dr}}^2/u^2))^{\frac{1}{2}}}{(1+(4\beta^2 v_{\mathrm{dr}}^2/u^2))^{\frac{1}{2}}}. \tag{4.6}$$

In (4.6) D_{p1} and D_{p3} are the particle eddy diffusivities normal to the drift direction. The eddy diffusivity along the particle drift direction is denoted D_{p2} in (4.6). The parameter β is the ratio of the product of the Lagrangian timescale of the fluid, T_{L}, and $\langle u^2\rangle^{\frac{1}{2}}$ to the longitudinal Eulerian integral lengthscale L_{f}, i.e.

$$\beta = \frac{\langle u^2\rangle^{\frac{1}{2}} T_{\mathrm{L}}}{L_{\mathrm{f}}}. \tag{4.7}$$

The factor of 4 appearing in (4.6) gives the correct limiting behaviour as $v_{\mathrm{dr}} \to 0$ and $v_{\mathrm{dr}} \to \infty$. For large values of the parameter v_{dr}/u' the continuity effect reduces the diffusivity in directions normal to drift by a factor of two relative to the diffusivity along the drift direction.

Asymptotic values of the eddy diffusivity measured from each of the reference times of the simulations are compared to Csanady's prediction, equation (4.6), in figure 11(*a*). The results in figure 11(*a*) show that the agreement between the simulation data and (4.6) is quite good for values of v_{dr}/u' less than about 2.5. For larger values of this parameter it can be observed from the figure that (4.6) underpredicts the measurements from the simulation. This discrepancy at large values of the drift velocity can be in part attributed to eddy decay and the fact that the Lagrangian velocity autocorrelation normal to the particle drift direction does not closely approximate the two-point spatial Eulerian correlation of lateral velocities. Examination of figure 10(*b*) shows that even for large values of the drift velocity this correlation does not possess significant regions containing negative loops. Other discrepancies between Csanady's prediction and the simulation data are due to such factors as the assumed form of the velocity autocorrelation. Csanady assumes the velocity autocorrelation to be a decaying exponential function. This functional form has been suggested by Hinze (1975) and used by other investigators (e.g. Picart, Berlemont & Gouesbet 1986). However, for low-Reynolds-number turbulence the decaying exponential function does not predict the autocorrelation as well as at higher Reynolds numbers (Yeung & Pope 1989).

Shown in figure 11(*b*) is the ratio of the asymptotic value of the eddy diffusivity of particles along the drift direction to the asymptotic eddy diffusivity of the fluid.

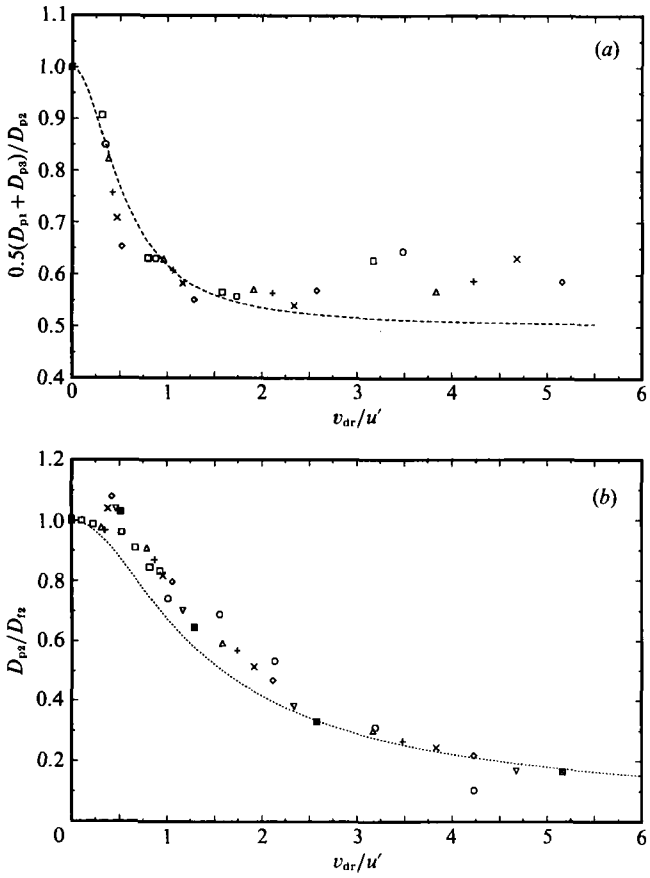

FIGURE 11. (*a*) Ratio of the asymptotic values of the eddy diffusivities in isotropic turbulence. □, $Re_\lambda = 32.3$; ○, $Re_\lambda = 30.8$; △, $Re_\lambda = 29.4$; +, $Re_\lambda = 28.0$; ×, $Re_\lambda = 26.7$; ◇, $Re_\lambda = 25.5$; ----, equation (4.7). (*b*) Ratio of the asymptotic values of the eddy diffusivities in isotropic turbulence. □, Wells & Stock (1983), 5 μm; ○, Wells & Stock (1983), 57 μm; △, $Re_\lambda = 32.3$; +, $Re_\lambda = 30.8$; ×, $Re_\lambda = 29.4$; ◇, $Re_\lambda = 28.0$; ▽, $Re_\lambda = 26.7$; ⊠, $Re_\lambda = 25.5$; ----, equation (4.9).

Also shown in this figure are the measurements from the experiment of Wells & Stock (1983) as well as the prediction of Csanady. For the asymptotic value of the diffusivity along the particle drift direction Csanady predicts

$$\frac{D_{p2}}{D_f} = \left(1+\frac{\beta^2 v_{dr}^2}{u^2}\right)^{-\frac{1}{2}}, \tag{4.8}$$

where D_{p2} is the particle eddy diffusivity along the drift direction and D_f is the asymptotic value of the fluid eddy diffusivity. Examination of figure 11(*b*) shows that agreement between the simulation data and the data of Wells & Stock is good and that (4.8) slightly under-predicts both the simulation and experimental measurements. It may also be seen from the figure that simulation measurements of D_{p2}/D_f are greater than unity for small values of the drift velocity. This may be in part due to the available sample from which the particle velocity correlations were computed, i.e. if the correlations could be computed by averaging over other simulations, it should be expected that D_{p2}/D_f would be less than unity for small drift velocities.

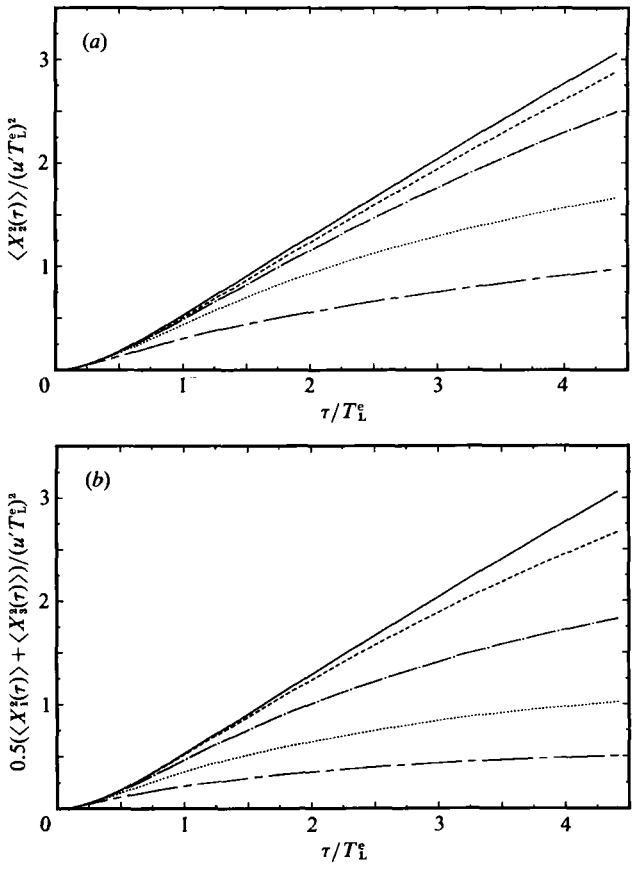

FIGURE 12. Effect of drift on the particle mean-square displacement, $Re_\lambda = 32.3$. (*a*) Drift component. (*b*) Normal components. ——, fluid; – – – –, $v_{dr}/u' = 0.32$, —·—, $v_{dr}/u' = 0.79$; · · · · · · · · ·, $v_{dr}/u' = 1.59$; — — —, $v_{dr}/u' = 3.17$.

The dispersion measurements for the drift cases are shown in figure 12. Consistent with the crossing-trajectories and continuity effect the particle dispersion is reduced as the drift velocity of the particle is increased. Comparison of these figures shows that the dispersion is decreased more in the directions normal to the drift direction than it is in the direction along particle drift.

Time histories of the eddy diffusivities for these cases are shown in figure 13. These figures show that as the drift velocity is increased the eddy diffusivity is decreased and it is also decreased unequally in the directions perpendicular and parallel to the particle drift. Figure 13 also shows that it is difficult to define an asymptotic diffusivity for the simulations of decaying isotropic turbulence. In contrast with the eddy diffusivities for particle dispersion in the absence of drift (figure 9*b*), the eddy diffusivities for these cases do not become time-independent at long diffusion times. This helps illustrate that the velocity and timescales experienced by the drifting particle are not the same as those experienced by a fluid element. This makes it quite difficult to apply a re-scaling of the variables in order to make the results representative of those obtained from stationary turbulence.

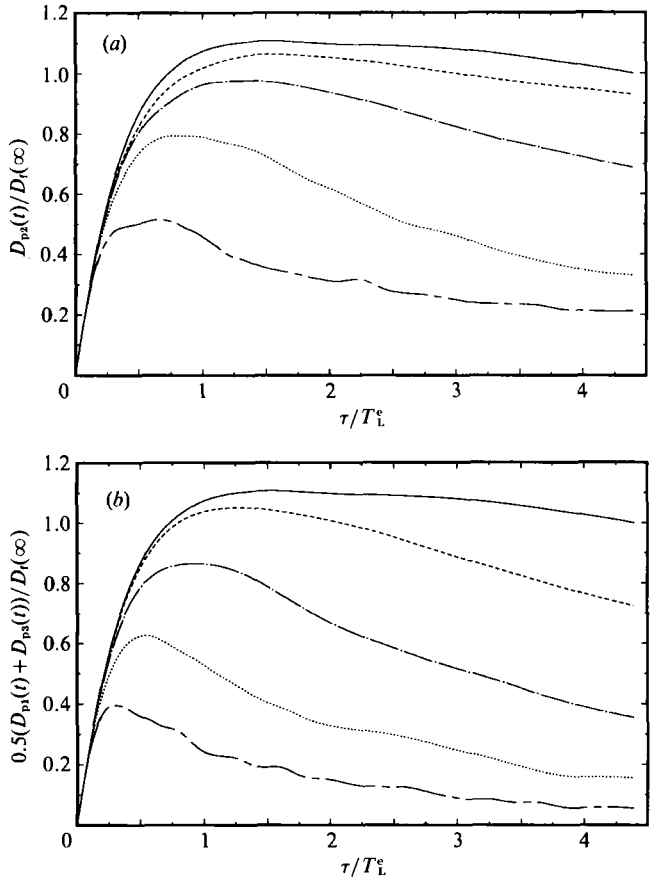

FIGURE 13. Effect of drift on the particle eddy diffusivity, $Re_\lambda = 32.3$. (*a*) Drift component. (*b*) Normal components. ——, fluid; – – – –, $v_{dr}/u' = 0.32$; —·—, $v_{dr}/u' = 0.79$; · · · · · · · · ·, $v_{dr}/u' = 1.59$; — — —, $v_{dr}/u' = 3.17$.

5. Dispersion in forced isotropic turbulence

Shown in figure 14(*a*) are the Lagrangian velocity autocorrelations obtained from simulations of forced isotropic turbulence for three values of the particle time constant. The velocity correlations obtained from the simulations of forced isotropic turbulence were computed using

$$R^{L}_{p\alpha\alpha}(\tau) = \frac{\langle v_\alpha(t)\, v_\alpha(t+\tau)\rangle}{\langle v^2(t)\rangle}. \tag{5.1}$$

The correlations presented in this section have been averaged over the three component directions ($\alpha = 1, 2$ and 3) and the time axis has been made dimensionless using the Lagrangian integral timescale of the fluid, T_L. The correlations shown in figure 14(*a*) are for particles in which the drift velocity is negligible. These figures illustrate the effect that increasing the particle inertia increases the particle 'memory' at its previous velocity, thus increasing its velocity autocorrelation. Similar results were also obtained from the simulations of decaying isotropic turbulence (see §4.1 and figure 8*a*). Figure 14(*b*) shows the velocity correlations of the fluid along the particle path for these particle time constants. This figure helps

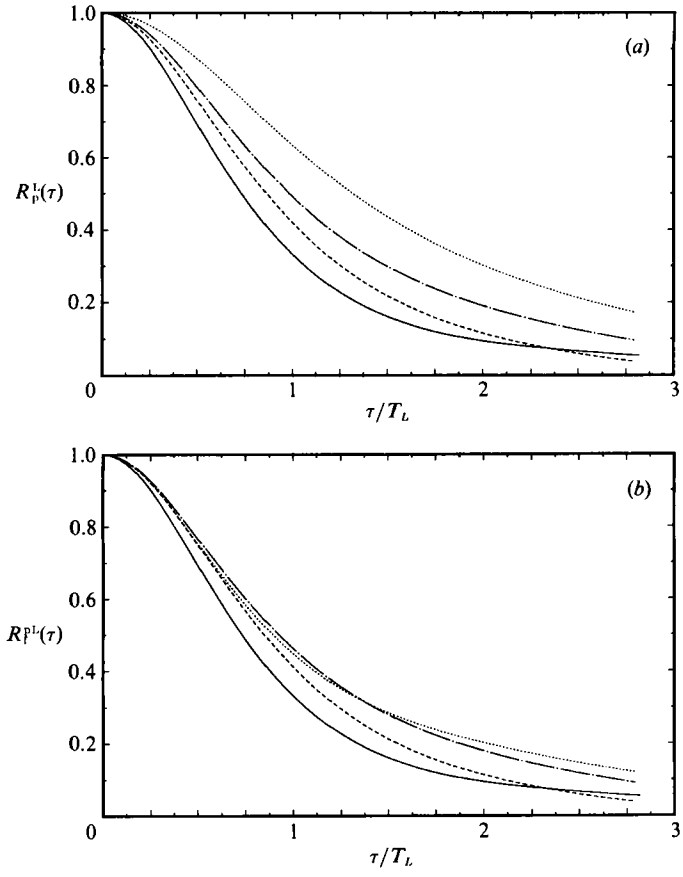

FIGURE 14. Effect of inertia on velocity correlations. (*a*) Particle velocity correlations. (*b*) Fluid velocity correlations along particle path. ——, fluid; – – –, $\tau_p/T_f = 0.075$; —·—, $\tau_p/T_f = 0.15$; ·····, $\tau_p/T_f = 0.52$.

τ_p/T_f	D_p/D_f^p	D_p/D_f
0.075	0.999	1.046
0.150	0.998	1.160
0.520	0.983	1.061

TABLE 7. Comparison of particle and fluid eddy diffusivities from stationary isotropic turbulence

to illustrate that the fluid neighbourhood sampled by the particle during its motion is dependent on its inertia since the fluid velocity correlations along the particle trajectory are different for each of the particle time constants used in the simulation.

Asymptotic eddy diffusivities were calculated using (2.3) and the results are summarized in table 7. In table 7 the value of D_p/D_f^p is the ratio of the eddy diffusivity of the particles to that of the fluid along the particle path. The quantity D_p/D_f is the ratio of the eddy diffusivity of the heavy particles to the eddy diffusivity of fluid elements. The quantity D_f is not dependent on the particle motion and therefore the particle inertia.

The values of D_p/D_f show that the asymptotic diffusivity of heavy particles is greater than that of fluid elements when the effect of particle drift is neglected. These

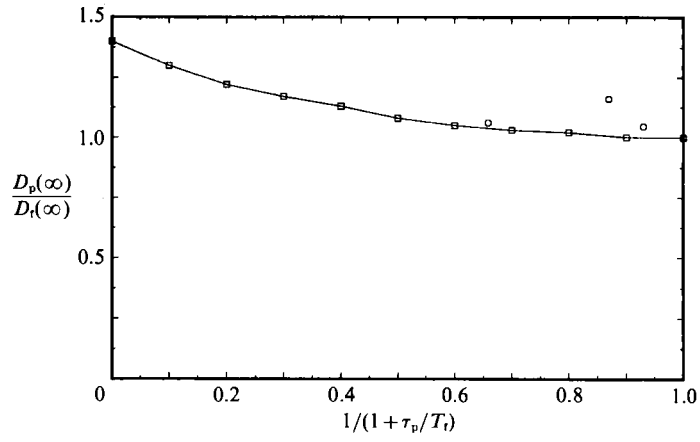

FIGURE 15. Effect of particle inertia on the asymptotic value of the eddy diffusivity in forced isotropic turbulence. □——□, Pismen & Nir (1978); ○, simulation results.

results are also consistent with those obtained from the simulations of decaying isotropic turbulence using heavy particles with the drift velocity set equal to zero (see §4.1 and figure 9*b*).

It can be seen from table 7 that the values of D_p/D_f^p are nearly equal to 1, with an increasing deviation from 1 for increasing particle inertia. The particle equation of motion may be used to interpret this result. In the absence of particle drift the equation of motion may be written as (see (3.13))

$$\tau_p \frac{dv}{dt} + v(t) = u(t), \tag{5.2}$$

considering for the moment the one-dimensional case.

As was shown in §2 this equation can be used to obtain a relationship between the power spectrum of the velocities of the particles and turbulence. This relationship is given in (2.8) and rewriting this for the one-dimensional case under discussion gives

$$(\tau_p^2\omega^2 + 1) E_p^L(\omega) = E_f^{pL}(\omega). \tag{5.3}$$

It was also shown in §2 that the long-time diffusivity is equal to the zeroth mode of the power spectrum. Using (5.3) it is clear that at long diffusion times

$$D_p(\infty) = D_f^p(\infty). \tag{5.4}$$

Based on this analysis it should be expected that the values of D_p/D_f^p would be identically equal to one if the simulation could be run for times long enough to approximate $t \to \infty$. This also explains the increasing deviation from one of this parameter for increasing particle inertia. Since the simulations were advanced the same number of timesteps the lighter particles travelled more particle time constants than the heavy particles and thus are closer to the long-time asymptote where $D_p/D_f^p = 1$. Finally, it is important to note that while (5.4) is not directly dependent upon the particle time constant, this does not imply that the particle eddy diffusivity is independent of particle inertia. The particle time constant influences the particle motion through (5.3) and therefore indirectly determines the eddy diffusivity, as can be observed in the values of D_p/D_f in table 7. Shown in figure 15 is a comparison of D_p/D_f obtained from the simulations with the results of Pismen & Nir (1978) who studied the dispersion of heavy particles using Corrsin's (1959) independence

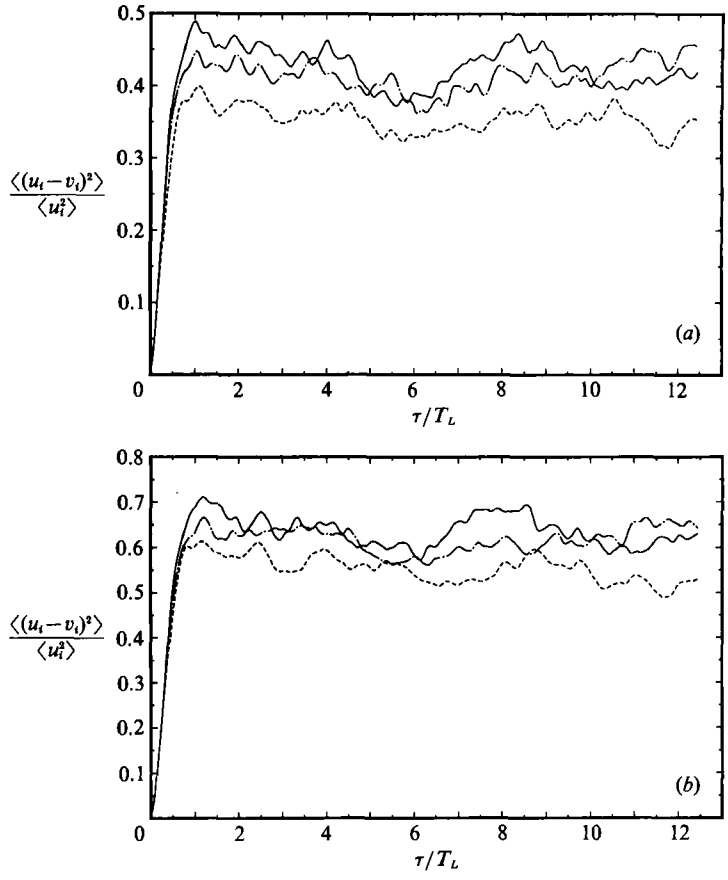

FIGURE 16. Time development of relative velocity, $v_{dr}/u' = 1.95$. (*a*) $\tau_p/T_f = 0.42$. (*b*) $\tau_p/T_f = 0.84$. ——, $i = 1$; – – – –, $i = 2$; —·—, $i = 3$.

approximation. As is evident from the figure, the simulation results are greater than the values predicted by Pismen & Nir, though the agreement is generally good. As is also evident from figure 15, Pismen & Nir found a monotonic increase in the eddy diffusivity for increasing particle time constants, unlike the results from the present simulations. This may reflect a sensitivity of this statistic to the sample of large-scale motions in the simulations of forced turbulence.

Two simulations were performed in which both the particle time constant and drift velocity were non-zero. As is also the case for particles where only the particle inertia is non-zero there is an adjustment period in which the particles are influenced by their initial conditions. Using the mean-square relative velocity difference as a measure of this adjustment period, figure 16 shows the time history of the quantity $\langle (u_i - v_i)^2 \rangle$ for the two cases used in the simulation. Figure 16(*a*) shows this quantity for the lighter particles and by comparison to figure 16(*b*) it may be observed this difference is less than for the heavy particles. Both figures 16(*a*) and 16(*b*) show the mean-square velocity difference $\langle (u_2 - v_2)^2 \rangle$ to be less than the other two velocity components. This difference is evidently due to the drift velocity being imposed in this direction only. The slight differences between the components of the mean-square relative velocity in the directions perpendicular to the drift direction are due to the slight anisotropy of the forcing scheme.

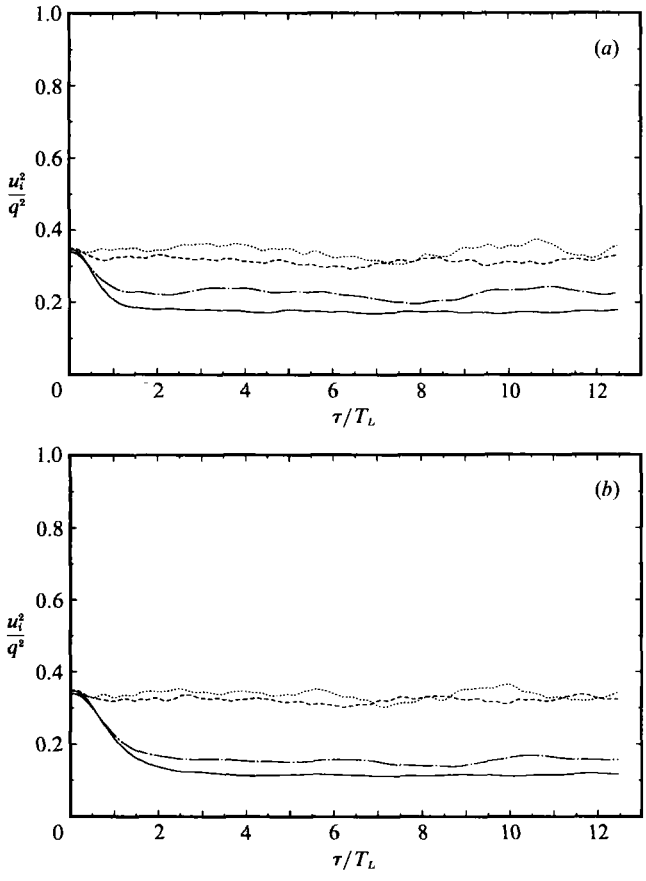

FIGURE 17. Time development of component energies, $v_{dr}/u' = 1.95$. (*a*) $\tau_p/T_f = 0.42$. (*b*) $\tau_p/T_f = 0.84$. ——, $i = 1, 3$ particles; – – –, $i = 1, 3$ fluid; —·—, $i = 2$ particles; ·····, $i = 2$ fluid.

τ_p/T_f	v_{dr}/u'	v_1^2/q_p^2	v_2^2/q_p^2	v_3^2/q_p^2
0.42	1.95	0.307	0.393	0.300
†0.42	1.95	0.31	0.38	0.31
0.84	1.95	0.303	0.401	0.296
†0.84	1.95	0.30	0.40	0.30

† Reeks (1977).

TABLE 8. Distribution of particle energies from stationary isotropic turbulence

Figure 17 shows the components of the particle and fluid kinetic energies for the two cases and the differences between the drift component and other velocity components is clear. For isotropic turbulence the distribution of energies among the three components of the fluid velocity is, of course, $\frac{1}{3}$. However, for particles in which the drift velocity and particle inertia are non-zero this is not the case. Table 8 shows the distribution of the particle kinctic energy among the velocity components corresponding to the statistically stationary portion of the simulation. These values show that the distribution of the energies among the components is nearly independent of particle inertia, depending only on the ratio of v_{dr}/u'. Also shown in

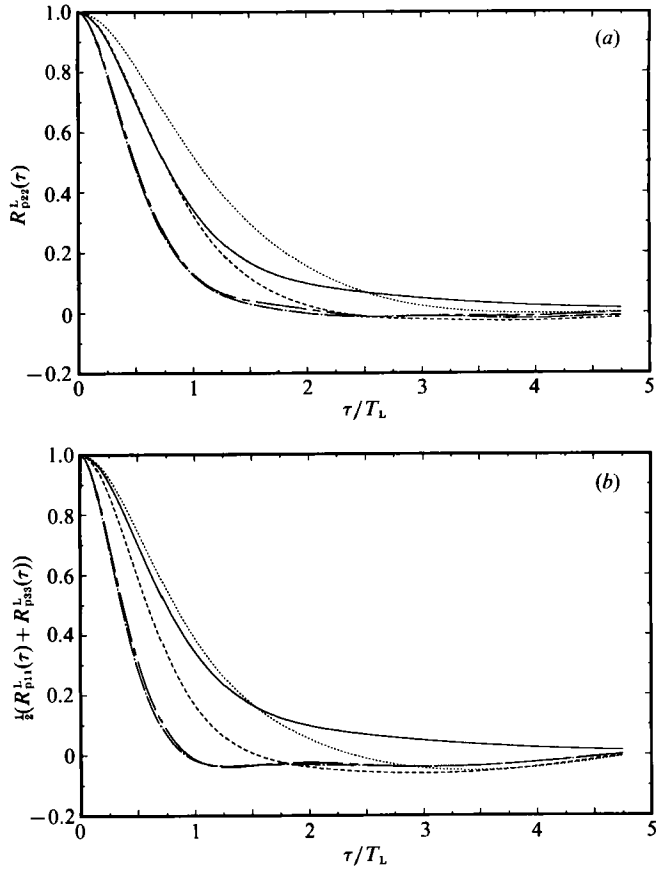

FIGURE 18. Effect of inertia on velocity correlations, $v_{dr}/u' = 1.95$. (*a*) Drift component. (*b*) Normal components. ——, fluid; – – – –, $\tau_p/T_f = 0.42$; —·—, fluid for $\tau_p/T_f = 0.42$; · · · · · · · · ·, $\tau_p/T_f = 0.84$; — — —, fluid for $\tau_p/T_f = 0.84$.

table 8 is an approximate comparison to a study by Reeks (1977). The comparison is approximate since Reeks did not show results for identical values of τ_p/T_f and v_{dr}/u' used in these simulations. However, there was not a wide variation of these ratios for this range of parameters in his study and thus the comparison is useful. It may be seen from table that the agreement between the simulation data and the results from Reeks' study is quite good.

Shown in figure 18 are the velocity autocorrelations of the particle velocities and the fluid velocities in the neighbourhood of the particle. Also shown for comparison is the velocity autocorrelation of fluid elements. Results from §(4.1) showed that increasing particle inertia increased the correlation of heavy particle velocities over that of fluid elements. Figure 18 shows that this effect is offset by the drift velocity of the particle. For the lighter particle ($\tau_p/T_f = 0.42$) the correlation of the velocities along the drift direction is nearly coincident with that of the fluid elements at small time separations. It may also be seen from these figures that the correlations of fluid velocities along the particle path are nearly the same for each of the particle time constants.

Time histories of the components of the eddy diffusivities are shown in figure 19. This figure illustrates the dramatic effect of the drift velocity on reducing the

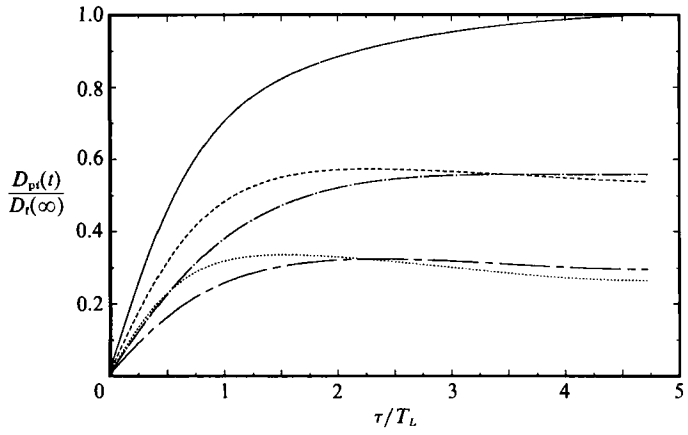

FIGURE 19. Effect of inertia on particle eddy diffusivity, $v_{dr}/u' = 1.95$. ——, fluid; – – – –, $i = 2$, $\tau_p/T_f = 0.42$; —·—, $i = 2$, $\tau_p/T_f = 0.84$; · · · · · · · · ·, $i = 1, 3$, $\tau_p/T_f = 0.42$; ——–, $i = 1, 3$, $\tau_p/T_f = 0.84$.

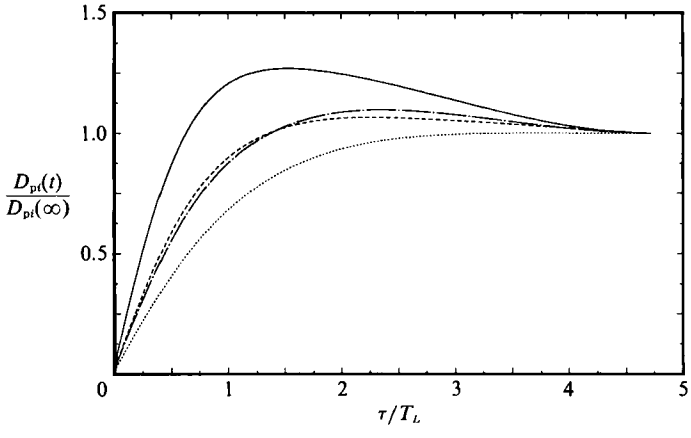

FIGURE 20. Effect of inertia on particle eddy diffusivity, $v_{dr}/u' = 1.95$. ——, $i = 1, 3$, $\tau_p/T_f = 0.42$; – – – –, $i = 2$, $\tau_p/T_f = 0.42$; —·—, $i = 1, 3$, $\tau_p/T_f = 0.84$; · · · · · · · · ·, $i = 2$, $\tau_p/T_f = 0.84$.

dispersion of heavy particles. For the values of τ_p/T_f used in these simulations it may be observed from the figure that the diffusivity is only weakly dependent on particle inertia. It can also be seen from figure 19 that the diffusivity in the directions normal to the drift direction is less than the diffusivity along the drift direction. These results are consistent with the crossing-trajectories and continuity effect.

Usually of interest in problems involving turbulent dispersion of heavy particles is the asymptotic value of the eddy diffusivity. The time history of $D_{pi}(t)/D_{pi}(\infty)$ is shown in figure 20. This figure shows that the components of the diffusivity normal to the drift direction can be greater than the asymptotic value for some values of time. This does not mean, however, that the particles disperse faster than fluid elements for these time intervals. Figure 19 shows that this is clearly not the case. It may also be seen from figure 20 that only a slight increase in the eddy diffusivity over the asymptotic value is attained for the components along the particle drift direction.

Some models of particle dispersion by turbulence are based on choosing functional forms of the Lagrangian velocity correlation of the fluid velocities along the particle path (see §2). Gouesbet *et al.* (1984) use such an approach and they recommend the following functional form for the velocity correlation:

$$R_f^{pL}(\tau) = \exp\left[\frac{-r}{(m^2+1)\,T_L^p}\right]\cos\left[\frac{mr}{(m^2+1)\,T_L^p}\right], \tag{5.5}$$

where the recommended value of the parameter m in (5.5) is $m = 1$. Gouesbet has shown that by using (5.5) it is possible that heavy particles will disperse faster than fluid elements. However, this analysis is derived in the framework of Tchen's theory for which the effect of an external body force is ignored. Since 'overshooting' is not allowed in Tchen's theory it seems unlikely that the correlation of fluid velocities along the particle path will have negative loops. None of the velocity correlations of the fluid along the particle path showed negative regions from the simulations. Picart *et al.* (1986) have used (5.5) along with a correction for the crossing-trajectories effect and obtained good agreement with Snyder & Lumley's (1971) data for particle dispersion in decaying isotropic turbulence. It should be remembered that the data of Snyder & Lumley is strongly influenced by the crossing-trajectories effect and therefore the form of the correction applied by Picart for crossing-trajectories may have been critical to the success of the model. This would seem to be especially true since the correction made for crossing trajectories does not account for the differences in dispersion in the vertical and horizontal planes. Since Picart could only check the dispersion transverse to the mean flow it seems likely that the dispersion in the other plane would be poorly predicted.

Finally, models that rely on the approach of specifying the functional form of the velocity autocorrelation along the particle path also require specification of the Lagrangian integral timescale. Picart *et al.* used a $k-\epsilon$ model to obtain the turbulence properties and specify the Lagrangian integral timescale as

$$T_{Li}^p \approx 0.20\frac{\langle u_i^2\rangle}{\epsilon}. \tag{5.6}$$

Application of (5.6) underpredicts the actual value of T_{L1}^p and T_{L3}^p from the simulations by a factor of 1.1 while T_{L2} is under predicted by a factor of 2.1. It should be remembered that T_{Li}^p in (5.6) is the Lagrangian integral timescale of the fluid elements along the particle path. Using (5.6) to calculate the Lagrangian integral timescale of fluid elements (independent of particle inertia or drift) underpredicts the actual value by a factor of 3.8. The integral timescale is also a function of v_{dr}/u' but (5.6) does not allow for any dependence of T_{Li}^p on this quantity. Therefore, the reasonable agreement between the predicted and measured values of T_{L1}^p and T_{L2}^p are most probably fortuitous. Equation (5.6) should not be expected to predict T_{L1}^p and T_{L3}^p as accurately for other ratios of v_{dr}/u'. Even with these shortcomings Picart *et al.* reported good agreement with both Snyder & Lumley's experiment and the data of Wells & Stock (1981).

6. Summary

The dispersion characteristics of heavy particles have been investigated using direct numerical simulation of decaying and forced isotropic turbulence. It was shown that, in the absence of an externally imposed body force, the dispersion of

particles in both decaying and forced isotropic turbulence is greater than that of fluid elements. It is important to note that the eddy diffusivity along the particle path is equal to that of heavy particles in the limit $t \to \infty$ for stationary turbulence. This was seen to be very nearly true in the simulations, especially for lighter particles. Increases in particle-eddy diffusivities relative to the fluid have also been reported in the analytical studies by Reeks (1977) and Pismen & Nir (1978). The increases in the particle-eddy diffusivity found in the present study were also in reasonable agreement with those reported by Reeks, and Pismen & Nir.

For applications in which the effect of particle inertia is negligible it was demonstrated that the effect of an externally imposed body force significantly reduces particle dispersion over that of fluid elements. It was also shown that because of the continuity effect, this reduction in particle dispersion is greater in directions normal to particle drift than parallel to the drift direction. Comparison of the simulation results with the Csanady's theory and the experimental measurements of Wells & Stock (1983) showed good agreement.

Lagrangian velocity correlations were found to exhibit negative regions only for cases in which the drift velocity is non-zero. Dispersion models that specify the functional form of the fluid velocity correlation along the particle trajectory should not be expected to perform well if the function allows for negative loops and particle drift is not significant.

The authors would like to thank Dr Robert Rogallo at the NASA-Ames Research Center for the use of his code and Dr Alan A. Wray of the NASA-Ames Research Center for his help with the VECTORAL compiler. This work was supported by the National Science Foundation (grant no. MEA-83-51417) and the Office of Naval Research who supported the first author with a graduate fellowship.

Appendix. Description of forcing scheme

Statistically stationary isotropic turbulence was obtained in the present study by forcing the low-wavenumber modes of the velocity field. The method used in this study was developed by Hunt *et al.* (1987) in their examination of the space–time structure of isotropic turbulence. In their scheme a steady, non-uniform force field is introduced at the large scale of the flow. Since the mean flow induced by the force is unstable, instabilities subsequently develop. This in turn leads to a chaotic structure with motions at all scales.

Symbolically, the addition of a forcing acceleration to the momentum equations may be expressed as

$$\frac{\hat{\mathrm{d}}u_i(\boldsymbol{k},t)}{\mathrm{d}t} = \hat{a}_i(\boldsymbol{k},t) + \hat{f}_i(\boldsymbol{k}), \tag{A 1}$$

where $\hat{u}_i(\boldsymbol{k},t)$ is the Fourier transform of the ith component of the velocity field at wavevector $\boldsymbol{k}$, $\hat{a}_i(\boldsymbol{k},t)$ is the Fourier transform of the rate of change of velocity with time from the Navier–Stokes equations, and $\hat{f}_i(\boldsymbol{k})$ is the acceleration due to the imposed force field.

The spectrum of the forcing coefficients was chosen to have contributions from values of $k = (14)^{\frac{1}{2}}$, i.e. $\boldsymbol{k} = (\pm 1, \pm 2, \pm 3)$, $(\pm 3, \pm 2, \pm 1)$, $(\pm 2, \pm 1, \pm 3)$, $(\pm 3, \pm 1, \pm 2)$, $(\pm 1, \pm 3, \pm 2)$. For a force field applied at this radius there are 24 combinations of the wavevector $\boldsymbol{k}$ whose magnitude is equal to $(14)^{\frac{1}{2}}$. Considering the Fourier

transform of the force field the real and imaginary parts of the three components of $\hat{\boldsymbol{f}}(\boldsymbol{k})$ yield 144 unknowns. Aside from the constraint that the moments of $\hat{\boldsymbol{f}}(\boldsymbol{k})$ be isotropic, additional constraints satisfied by the force field were

$$\boldsymbol{k}\cdot\hat{\boldsymbol{f}} = 0, \tag{A 2}$$

and

$$\hat{f}_i\hat{f}_i^* = 1. \tag{A 3}$$

Equation (A 2) constrains the force field to be solenoidal and therefore avoid the generation of large pressure fluctuations. Equation (A 3) was enforced for each wavevector $\boldsymbol{k}$ such that $|\boldsymbol{k}| = (14)^{\frac{1}{2}}$.

For a force field applied at $|\boldsymbol{k}| = (14)^{\frac{1}{2}}$ the moments of $\hat{\boldsymbol{f}}(\boldsymbol{k})$ up to fourth order may be constrained to satisfy isotropy. These constraints along with (A 2) and (A 3) yield a nonlinear system of 144 equations. This system of equations was then solved for the Fourier coefficients of the force field using the Polak–Ribiere conjugate gradient method (see Press *et al.* 1987).

REFERENCES

Batchelor, G. K. 1949 Diffusion in a field of homogeneous turbulence. *Austral. J. Sci. Res.* **2**, 437–450.

Calabrese, R. V. & Middleman, S. 1979 The dispersion of discrete particles in a turbulent fluid field. *AIChE J.* **25**, 1025–1035.

Cooley, J. W. & Tukey, J. W. 1965 An algorithm for the machine calculation of complex Fourier series. *Maths Comput.* **19**, 297–301.

Corrsin, S. 1953 Remarks on turbulent heat transfer. *Proc. of the Iowa Thermodynamics Symp. University of Iowa*, pp. 5–30.

Corrsin, S. 1959 Progress report on some turbulent diffusion research. From Proceedings of the International Symposium on Atmospheric Diffusion and Air Pollution, *Adv. Geophys.* **6**, 161–164.

Corrsin, S. 1961 Theories of turbulent dispersion. *Mécanique de la Turbulence*, Colloques Internationaux du Centre National de la Recherche Scientifique, no. 108, Editions du CNRS, Paris, pp. 27–52.

Csanady, G. T. 1963 Turbulent diffusion of heavy particles in the atmosphere. *J. Atmos. Sci.* **20**, pp. 201–208.

Eswaran, V. & Pope, S. B. 1988 An examination of forcing in direct numerical simulations of turbulence. *Computers Fluids* **16**, 257–278.

Elghobashi, S. E. & Truesdell, G. C. 1989 Direct simulation of particle dispersion in a decaying grid turbulence. Presented at *Seventh Symp. on Turbulent Shear Flows, Stanford University*, California.

Frenkiel, F. N. 1953 Turbulent diffusion: mean concentration distribution in a flow field of homogeneous turbulence. *Adv. Appl. Mech.* **3**, 61–107.

Fung, J. & Perkins, R. J. 1989 Particle trajectories in turbulent flow generated by true-varying random Fourier modes. *Proc. Adv. in Turbulence 2* (ed. H. H. Fernholz & H. E. Fiedler), pp. 322–328. Springer.

Gottlieb, D. & Orszag, S. A. 1977 *Numerical analysis of spectral methods: theory and applications.* CBMS-NSF Regional Conference series in applied mathematics, vol. 26, SIAM, Philadelphia, Pennsylvania.

Gouesbet, G., Berlemont, A. & Picart, A. 1984 Dispersion of discrete particles by continuous turbulent motions. Extensive discussion of the Tchen's theory, using a two-parameter family of Lagrangian correlation functions. *Phys. Fluids* **27**, 827–837.

Grant, H. L., Stewart, R. W. & Moilliet, A. 1962 Turbulence spectra from a tidal channel. *J. Fluid Mech.* **12**, 241–268.

Hinze, J. O. 1975 *Turbulence.* McGraw-Hill.

Hunt, J. C. R., Buell, J. C. & Wray, A. A. 1987 Big whorls carry little whorls. *Proc. of the 1987 Summer Program, Rep.* CTR-S87, Stanford University, California.

LEE, C. L., SQUIRES, K. D., BERTOGLIO, J. P. & FERZIGER, J. H. 1988 Study of Lagrangian characteristic times using direct numerical simulation of turbulence. *Turbulent Shear Flows 6* (ed. B. E. Launder *et al.*), pp. 58–67. Springer.

LEE, M. J. & REYNOLDS, W. C. 1985 Numerical experiments on the structure of homogeneous turbulence. *Dept Mech. Engng Rep.* TF-24, Stanford University, California.

LUMLEY, J. L. 1957 Some problems connected with the motion of small particles in turbulent fluid. Ph.D. dissertation, The Johns Hopkins University, Baltimore, Maryland.

LUMLEY, J. L. 1961 The mathematical nature of the problem relating Lagrangian and Eulerian statistical functions in turbulence. *Mécanique de la Turbulence*, Colloques Internationaux du Centre National de la Recherche Scientifique, no. 108, Editions du CNRS, Paris, pp. 17–26.

MCLAUGHLIN, J. B. 1989 Aerosol particle deposition in numerically simulated channel flow. *Phys. Fluids* **1**, 1211–1224.

MAXEY, M. R. 1987 The gravitational settling of aerosol particles in homogeneous turbulence and random flow fields. *J. Fluid Mech.* **174**, 441–465.

MAXEY, M. R. & RILEY, J. J. 1983 Equation of motion for a small rigid sphere in a nonuniform flow. *Phys. Fluids* **26**, 883–889.

MEEK, C. C. & JONES, B. G. 1973 Studies of the behavior of heavy particles in a turbulent fluid flow. *J. Atmos. Sci.* **30**, 239–244.

NIR, A. & PISMEN, L. M. 1979 The effect of a steady drift on the dispersion of a particle in turbulent fluid. *J. Fluid Mech.* **94**, 369–381.

PICART, A., BERLEMONT, A. & GOUESBET, G. 1986 Modeling and predicting turbulence fields and the dispersion of discrete particles transported by turbulent fields. *Intl J. Multiphase Flow* **12**, 237–261.

PISMEN, L. M. & NIR, A. 1978 On the motion of suspended particles in stationary homogeneous turbulence. *J. Fluid Mech.* **84**, 193–206.

PRESS, W. H., FLANNERY, B. P., TEUKOLSKY, S. A. & VETTERLING, W. T. 1987 *Numerical Recipes*. Cambridge University Press.

PRUPPACHER, H. R. & KLETT, J. D. 1978 *Microphysics of Clouds in precipitation*. Reidel.

REEKS, M. W. 1977 On the dispersion of small particles suspended in an isotropic turbulent field. *J. Fluid Mech.* **83**, 529–546.

RILEY, J. J. 1971 Computer simulations of turbulent dispersion. Ph.D. dissertation, The Johns Hopkins University, Baltimore, Maryland.

RILEY, J. J. & PATTERSON, G. S. 1974 Diffusion experiments with numerically integrated isotropic turbulence. *Phys. Fluids* **17**, 292–297.

ROGALLO, R. S. 1981 Numerical experiments in homogeneous turbulence. *NASA Tech. Memo.* 81315.

SATO, Y. & YAMAMOTO, K. 1987 Lagrangian measurement of fluid particle motion in an isotropic turbulent field. *J. Fluid Mech.* **175**, 183–199.

SHLIEN, D. J. & CORRSIN, S. 1974 A measurement of the Lagrangian velocity autocorrelation in approximately isotropic turbulence. *J. Fluid Mech.* **62**, 255–271.

SNYDER, W. H. & LUMLEY, J. L. 1971 Some measurements of particle velocity autocorrelation functions in a turbulent flow. *J. Fluid Mech.* **48**, 41–71.

SQUIRES, K. D. & EATON, J. K. 1990 Particle response and turbulence modification in isotropic turbulence. *Phys. Fluids* A **2**, 1191–1203.

SQUIRES, K. D. & EATON, J. K. 1991 Lagrangian and Eulerian statistics obtained from direct numerical simulations of homogeneous turbulence. *Phys. Fluids* A **3**, 130–143.

STAPOUNTZIS, H., SAWFORD, B. L., HUNT, J. C. R. & BRITTER, R. E. 1988 Structure of the temperature field downwind of a line source in grid turbulence. *J. Fluid Mech.* **165**, 401–424.

TAVOULARIS, S., BENNETT, J. C. & CORRSIN, S. 1978 Velocity derivative skewness in small Reynolds number, nearly isotropic turbulence. *J. Fluid Mech.* **88**, 63–69.

TAYLOR, G. I. 1921 Diffusion by continuous movements. *Proc. R. Soc. Lond.* A **20**, 196–211.

TAYLOR, G. I. 1935 Statistical theory of turbulence. *Proc. R. Soc. Lond.* A **151**, 421–478.

TCHEN, C. M. 1947 Mean value and correlation problems connected with the motion of small particles suspended in a turbulent fluid. Ph.D. dissertation, University of Delft, The Hague.

TENNEKES, H. L. 1975 Eulerian and Lagrangian time microscales in isotropic turbulence. *J. Fluid Mech.* **67**, 561–567.

TOWNSEND, A. A. 1954 The diffusion behind a line source in homogeneous turbulence. *Proc. R. Soc. Lond.* A **224**, 487–512.

WARHAFT, Z. 1984 The interference of thermal fields from line sources in grid turbulence. *J. Fluid Mech.* **144**, 363–387.

WELLS, M. R. & STOCK, D. E. 1983 The effects of crossing trajectories on the dispersion of particles in a turbulent flow. *J. Fluid Mech.* **136**, 31–62.

YEUNG, P. K. & POPE, S. B. 1988 *J. Comput. Phys.* **79**, 373.

YEUNG, P. K. & POPE, S. B. 1989 Lagrangian statistics from direct numerical simulations of isotropic turbulence. *J. Fluid Mech.* **207**, 531–586.

YUDINE, M. I. 1959 Physical considerations on heavy particle diffusion. From Proceedings of the International Symposium on Atmospheric Diffusion and Air Pollution, *Adv. Geophys.* **6**, 185–191.